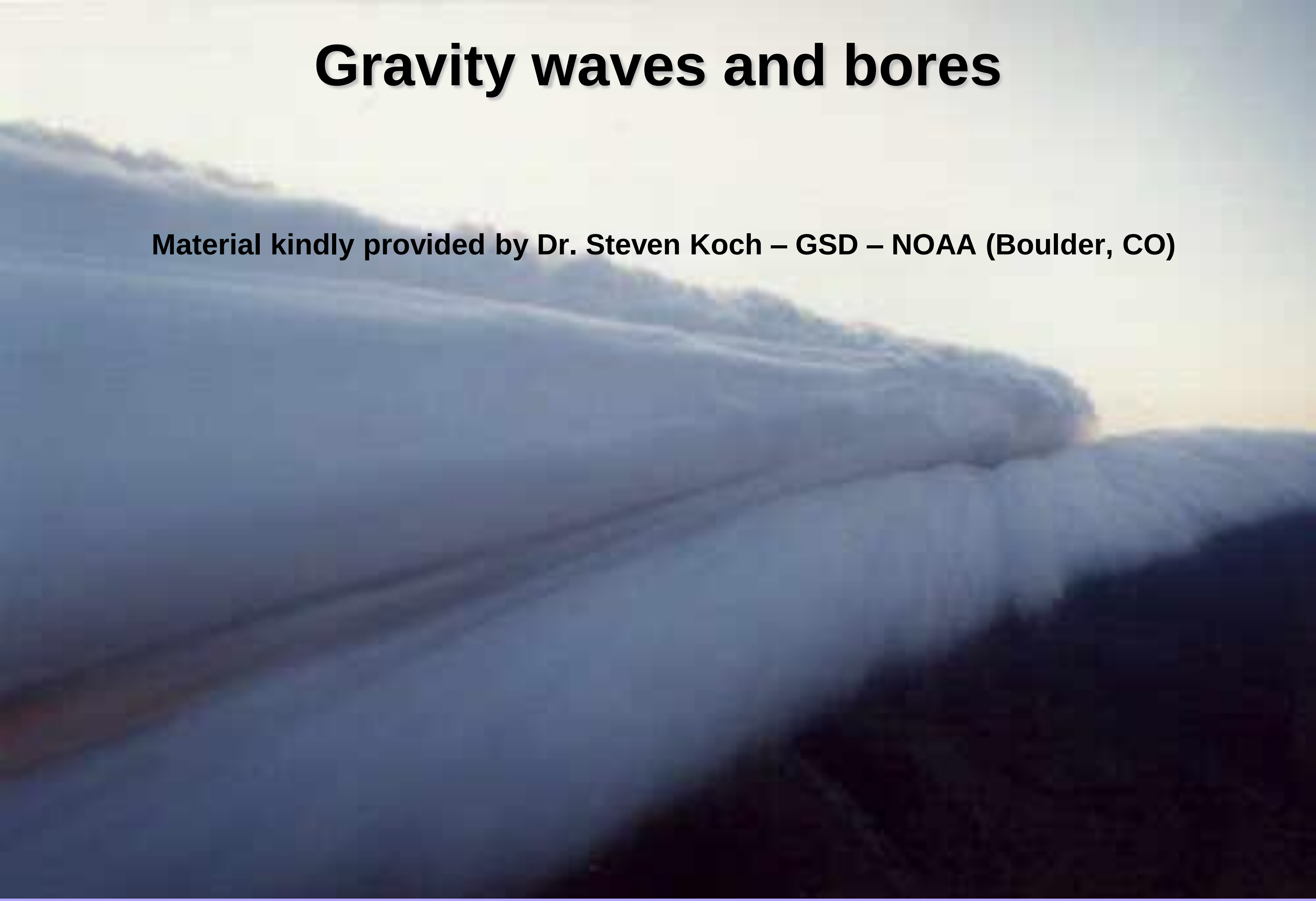

Gravity waves and bores

Material kindly provided by Dr. Steven Koch – GSD – NOAA (Boulder, CO)

Presented at Iowa State University
11 April 2005

What is a gravity wave?

An oscillation caused by the displacement of an air parcel which is restored to its initial position by gravity. The lifting force is buoyancy, while the restoring force is gravity.

- The time it takes for the air parcel to move back to its starting point after being displaced is called the buoyancy period.

$$\tau_B = 2\pi \sqrt{\frac{1}{\frac{g}{T}\left(\Gamma_d - \Gamma\right)}}$$

- The buoyancy period increases as the atmosphere becomes more unstable, because if you displace an air parcel it will oscillate farther from the equilibrium position; thus, it will take longer and longer for the return trip than it would in a stable atmosphere. When the atmosphere is unstable the displaced air parcel will never return and the buoyancy period is infinitely large.

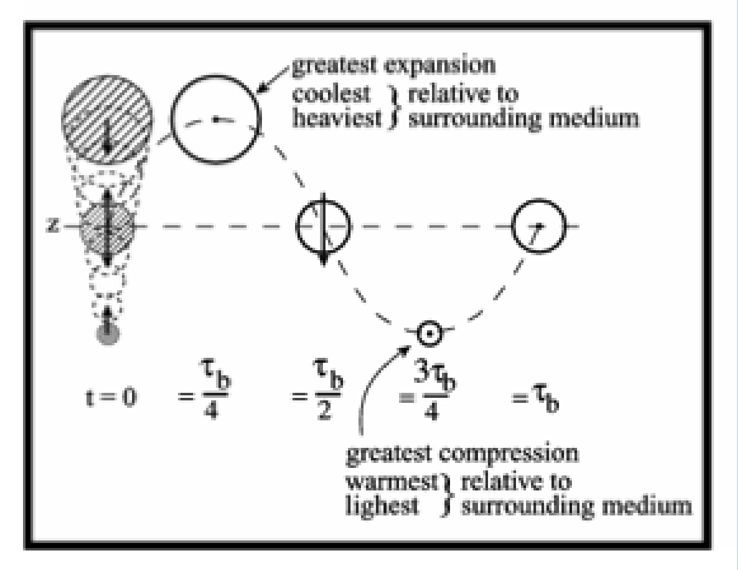

Gravity waves are typically dispersive

- **For** nondispersive **waves: the pattern in the lower part of the diagram propagates without change of shape**
- **For** dispersive **waves: the shape of the pattern changes in time as the individual waves propagate through the packet.**

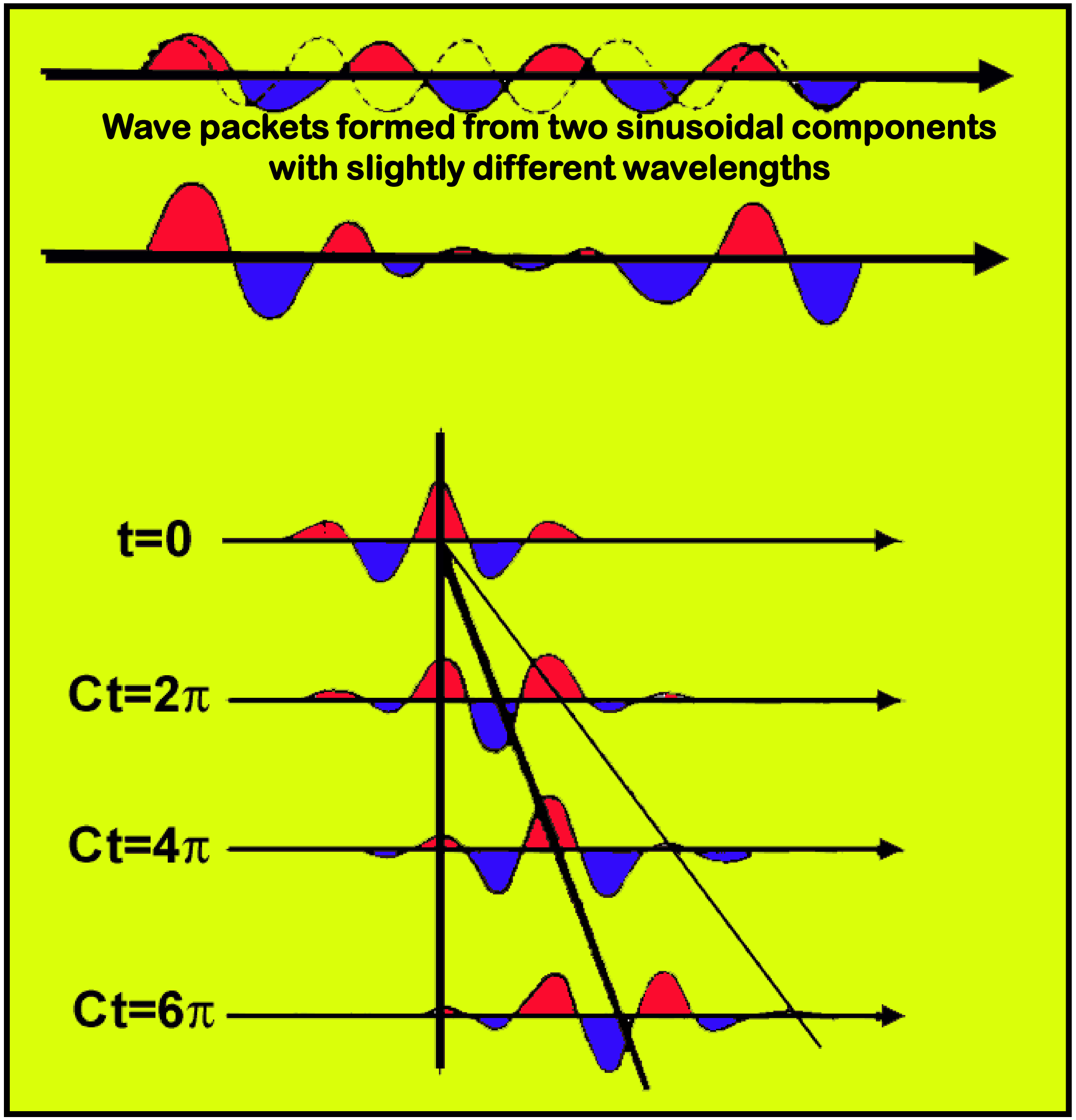

Gravity Currents in Geophysical Flows

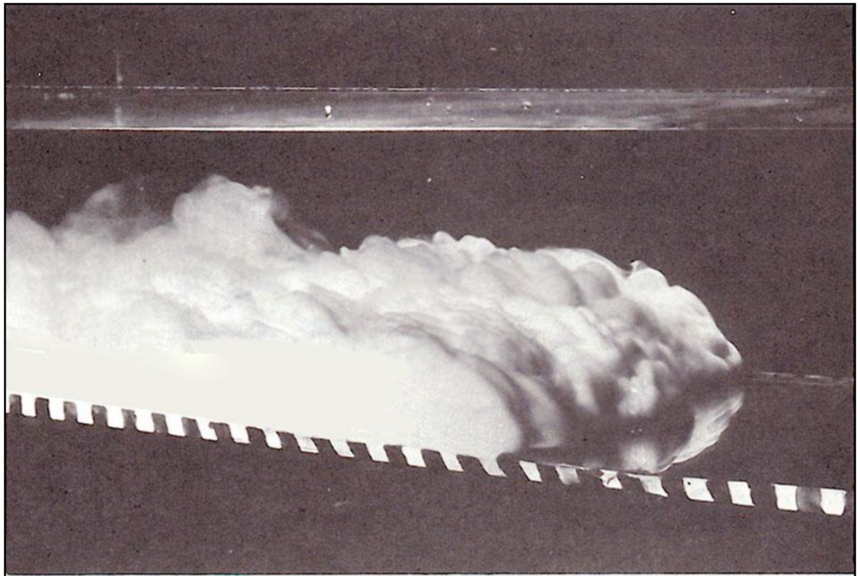

Lobes and clefts within the frontal region of a gravity current of salt water along the floor of a freshwater tank (Simpson 1987)

A gravity current is a mass flow driven by a horizontal pressure gradient as a denser fluid intrudes into a less dense fluid.

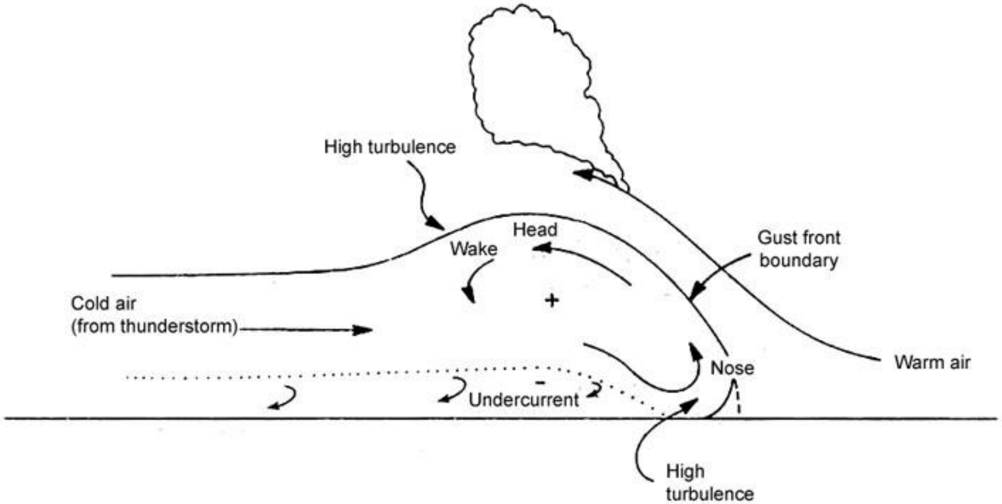

Schematic diagram of thunderstorm outflow, a type of gravity current (after Goff 1976)

Powder snow avalanche gravity current (Simpson 1987)

Wave polarization relationships

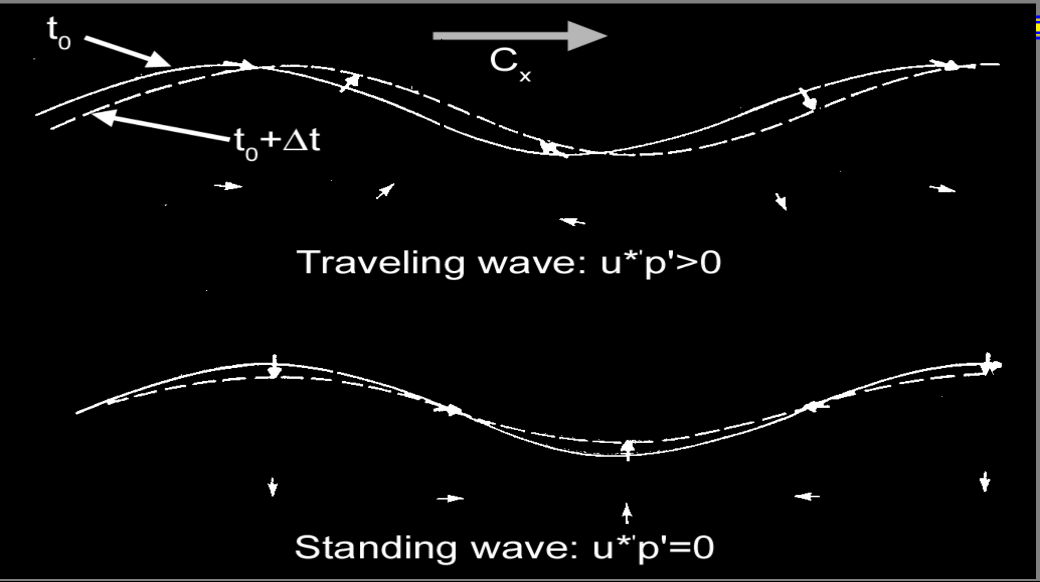

Propagating gravity waves display strong covariance between the wave-normal wind component u* and the pressure perturbation p'

Upward motion and clouds are found ahead of the mesohigh at the "nodal point" for "internal" waves displaying an upstream tilt.

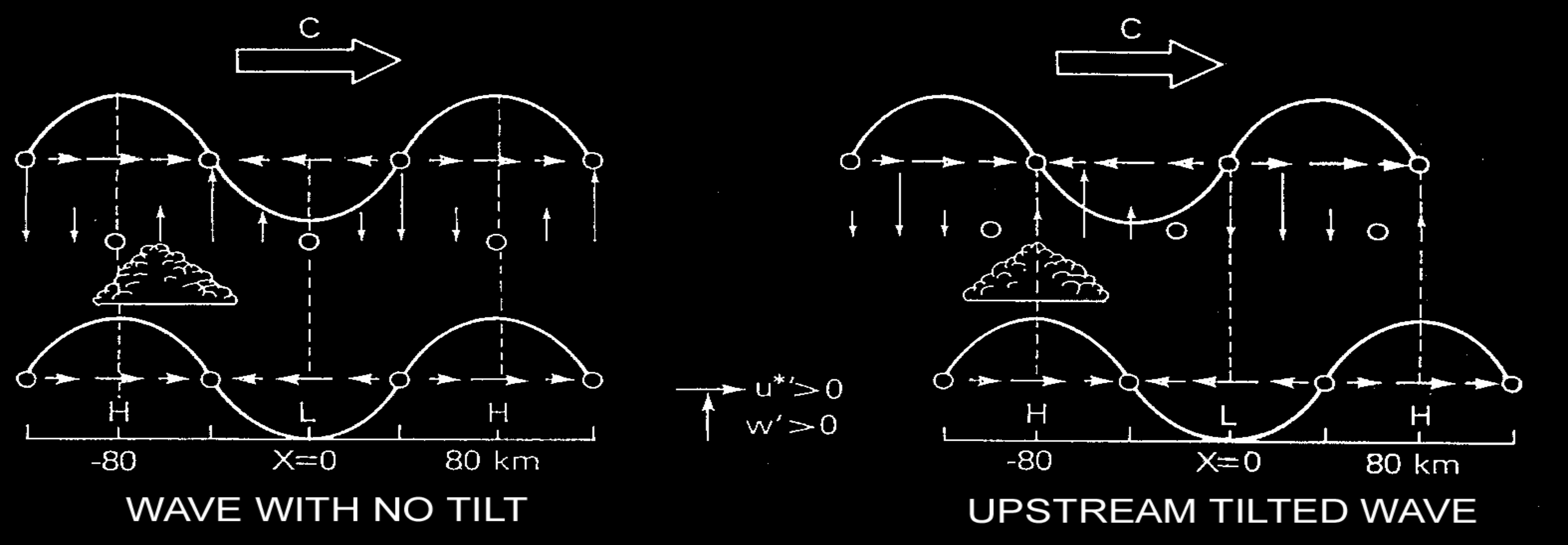

WAVE DUCTING

According to the dispersion equation, upward propagating (internal) waves in the absence of the Coriolis force (*f = 0*) and assuming plane waves (*l = 0*) can only occur if $\nu < N$. Otherwise, they are "evanescent".

$$m^2 = \left(\frac{N}{\nu}\right)^2 k^2 = \left[\frac{N}{k(C-U)}\right]^2 k^2 = \left(\frac{N}{C-U}\right)^2$$

At the "critical level", where $C = U$, the waves are "trapped" from further upward propagation as the vertical wavenumber m becomes infinite.

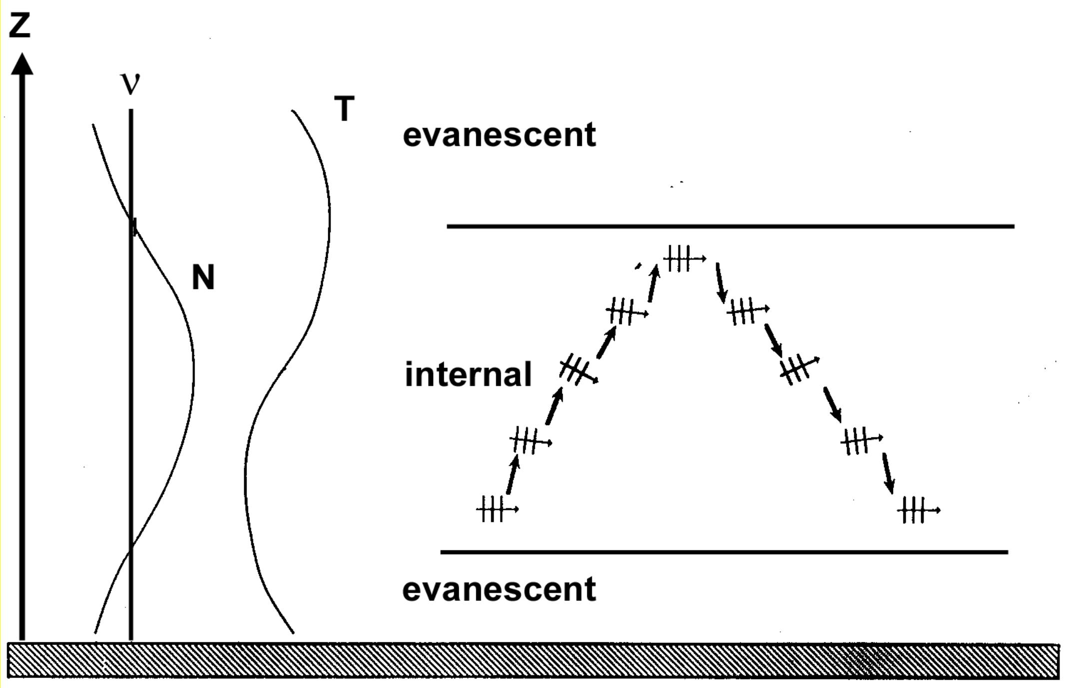

Phase speed: $C\text{-}U = \nu / k$

The internal layer represents a "wave duct". However, this stable layer must be thick enough to accommodate 1/4 of the vertical wavelength. Also, at the critical level, the Richardson Number must be small (<0.25).

THE CLASSIC WAVE DUCT SOUNDING

$$C_d = \frac{D_1 N_1}{\pi\left(0.5 + n\right)}$$

Note: This sounding is also conducive to occurrence of elevated convection

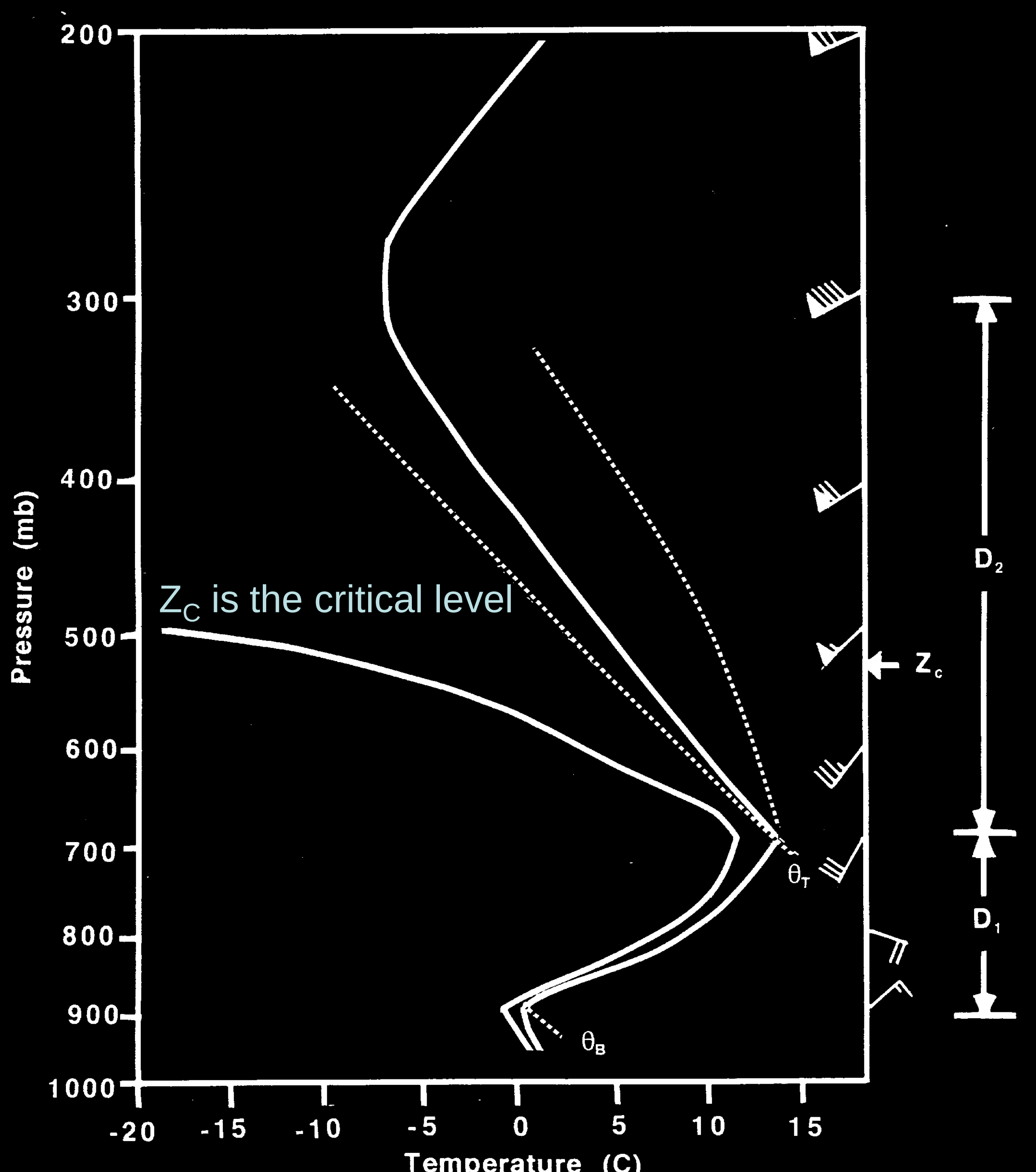

Schematic representation of a Ducted Gravity Wave with ½ vertical wavelength trapped between the ground and a Critical Level (Ralph et al. 1993)

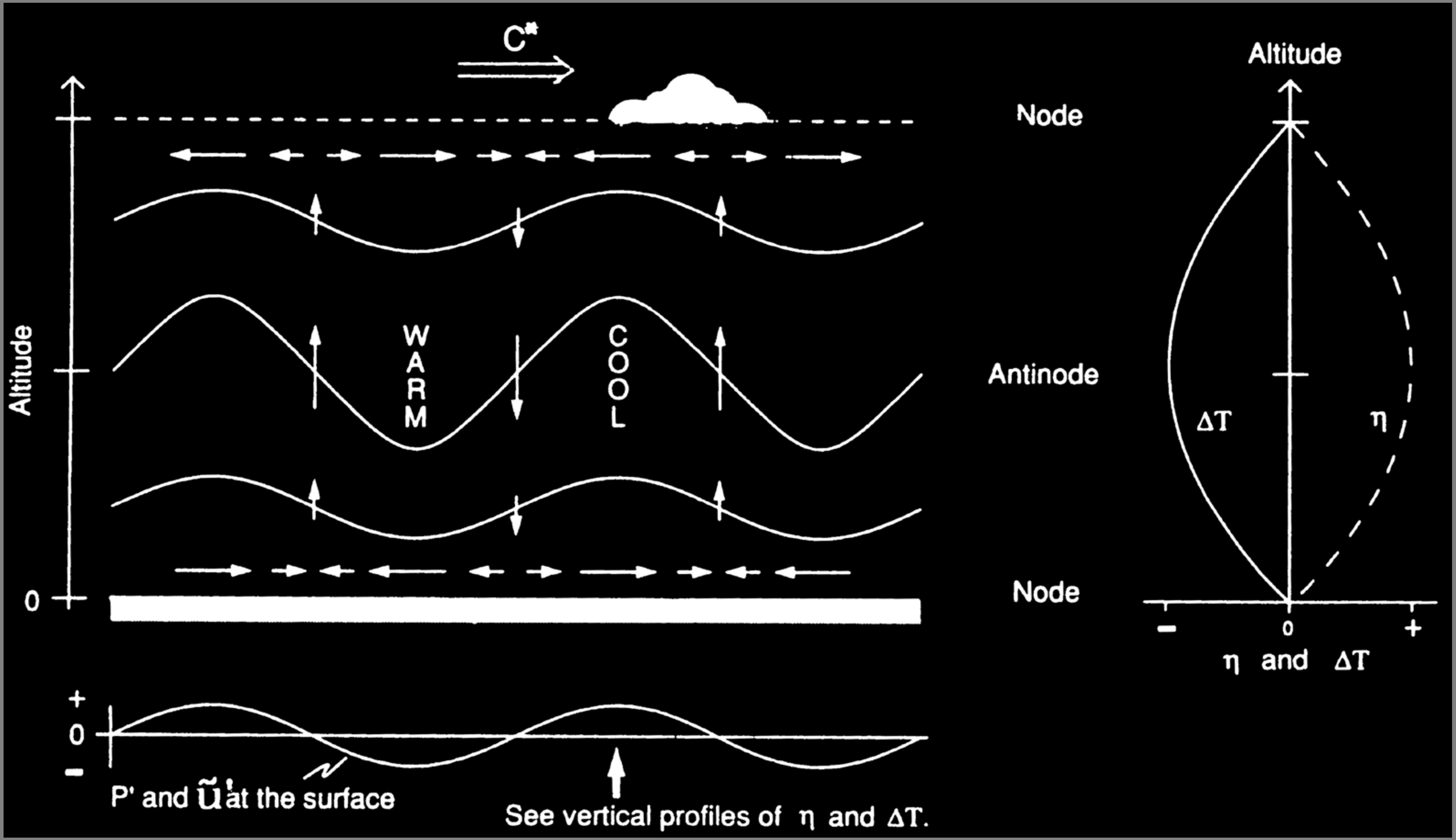

Evolution of a Gravity Current into a Bore

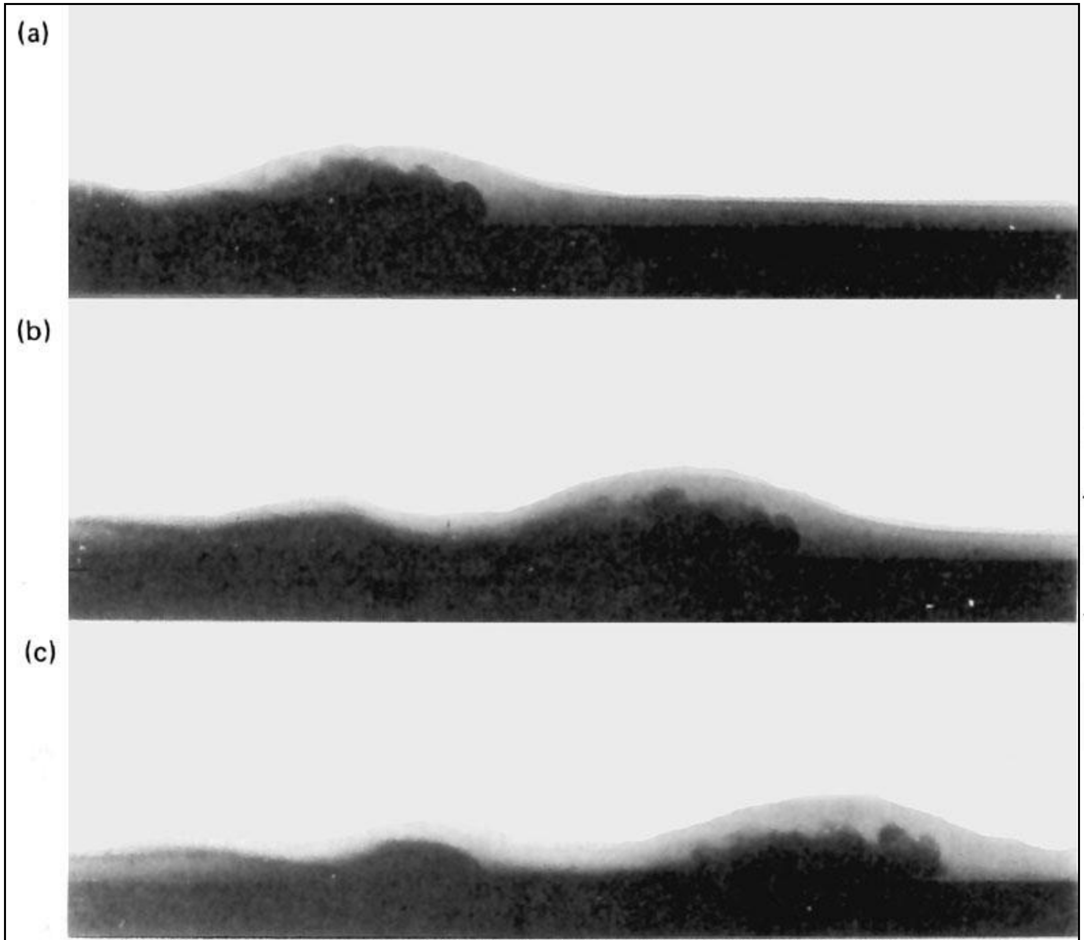

Evolution of an undular bore from an advancing gravity current (Simpson 1987). Fluid enveloping the current is similar to what happens to warm air underneath a low-level inversion as a gravity current intrudes into the inversion.

An internal bore in the atmosphere is a hydraulic jump, a type of gravity wave generated by the intrusion of a gravity current into a low-level stable layer.

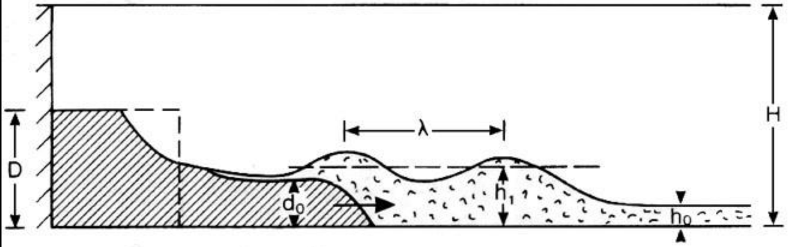

Generation of an internal bore of depth h_1 by an advancing gravity current of depth d_0 intruding into a stable layer of depth h_0

Passage of the bore results in a sustained elevation of the stable layer. Unlike gravity currents, bores do not transport mass.

Evolution of a Bore into a Soliton

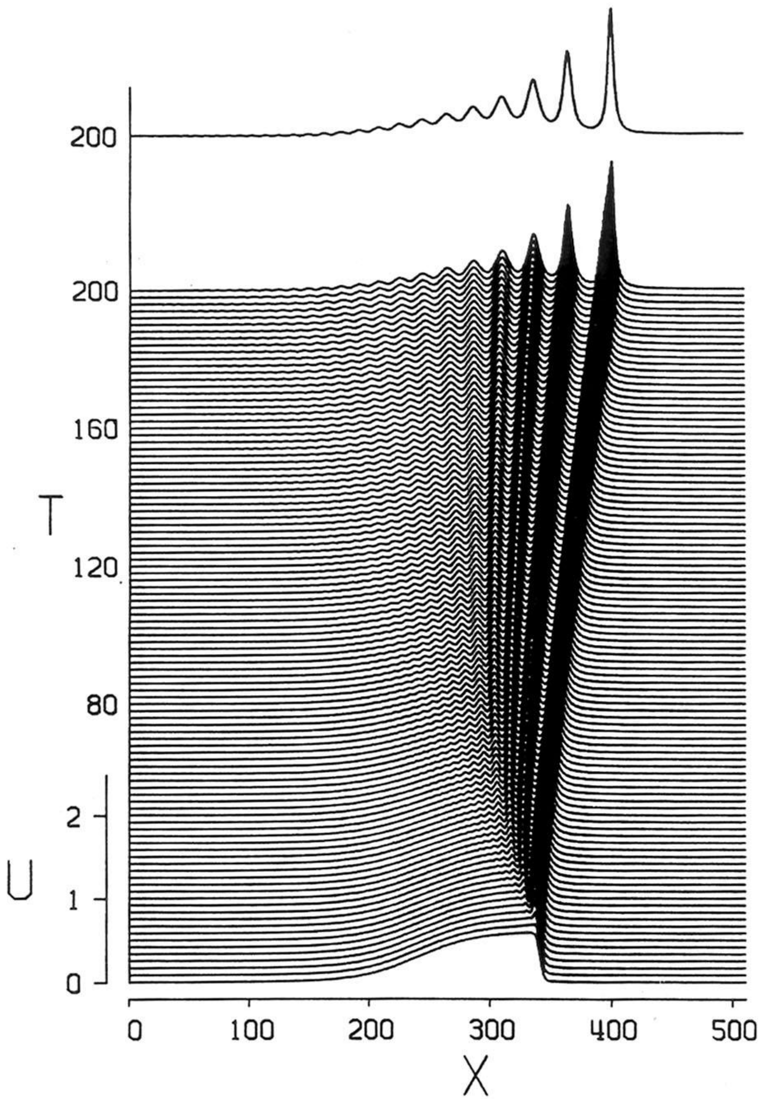

Solution of the BDO equation for deep-fluid solitary waves from an initial wave of elevation along an inversion in a waveguide embedded in a neutrally stable fluid of infinite extent (Christie 1989)

A train of amplitude-ordered solitary waves (or soliton) can evolve from bores in some instances. Wave amplitudes vary inversely with their width and are highly dispersive.

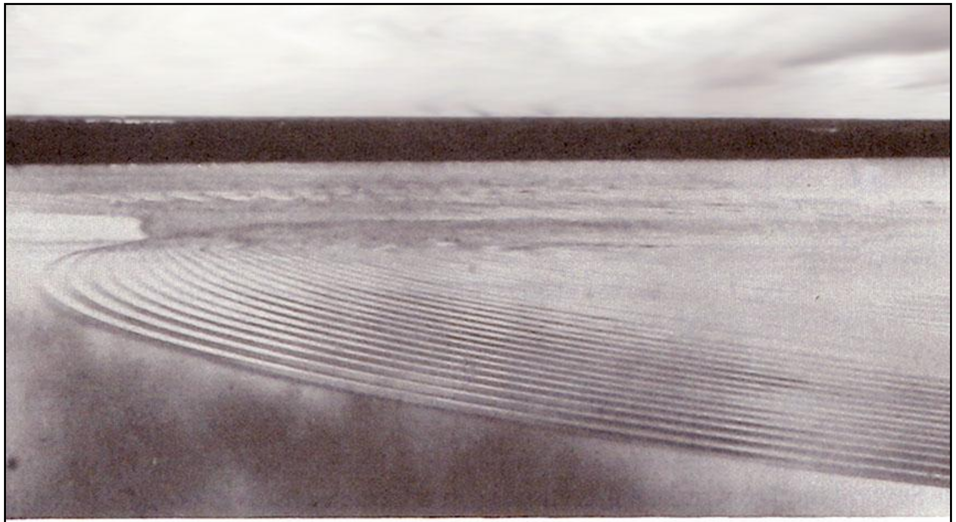

Tidal bore at the mouth of the Araguari River, in Brazil. The bore is undular, with over 20 waves visible (Courtesy of D. K. Lynch, in Simpson 1987)

The number of waves increases with time, but is limited by turbulent dissipation. The energy of the wave system tends to be concentrated in the first few solitary waves.

Bore Strength (Hydraulic Theory)

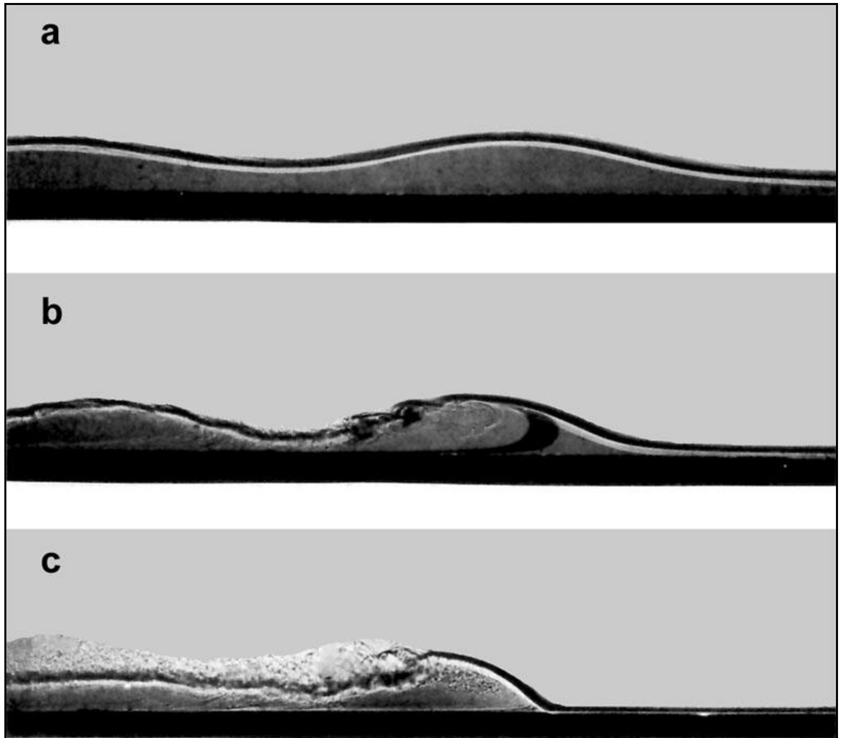

Transition of an undular bore to a turbulent bore at an interface between two fluids as bore strength increases from 1.5 to 3.0 to >4.0

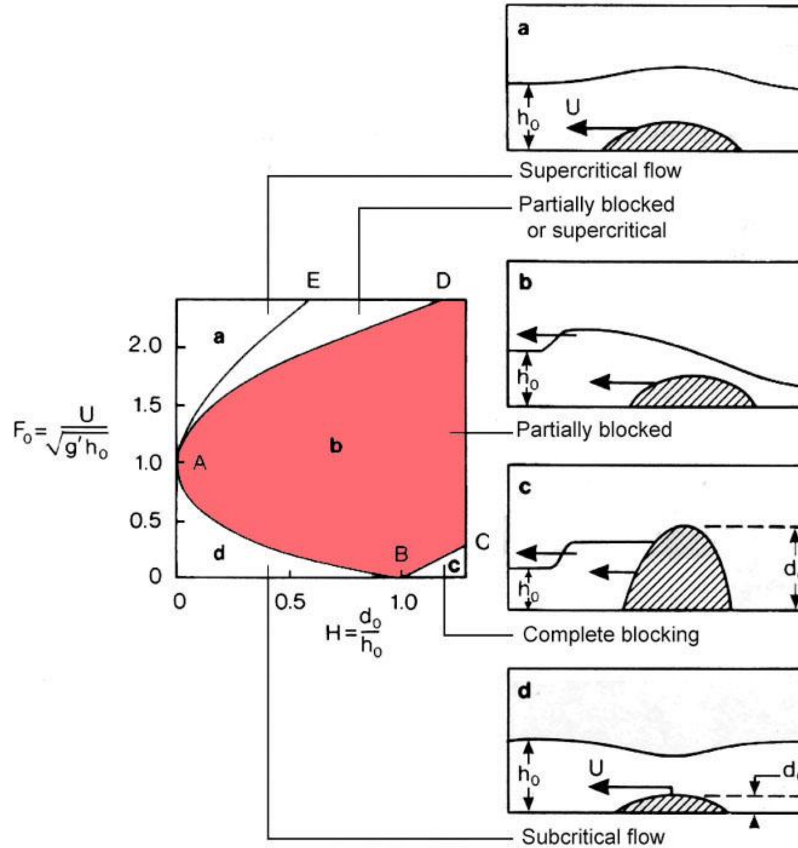

Four types of disturbances that can be generated by a moving obstacle at the interface between two fluids (hydraulic theory)

Transition of an <u>undular</u> bore into a <u>turbulent</u> bore depends upon its strength (d_b / h_0). Bore strength is determined by the Froude Number and the ratio of the gravity current depth to the inversion depth (d_0 / h_0)

Houghton and Kasahara (1968)

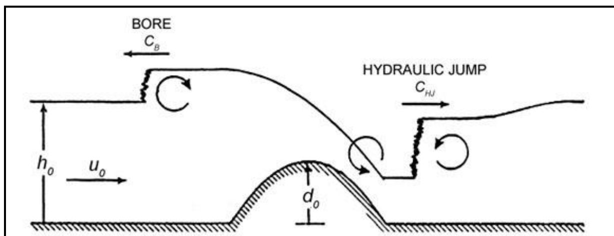

Schematic of shallow-water flow over a barrier depicting the upstream-propagating bore and downstream-propagating jump (Klemp et al. 1997)

Theory

(Rottman and Simpson 1989; Haase and Smith 1989)

- **Bore speed of propagation**

$$C_{bore} = C_{gw}\sqrt{0.5\left(d_b/h_0\right)\left(1+d_b/h_0\right)}$$
$$= Nh_0\left[0.5\left(d_b/h_0\right)\left(1+d_b/h_0\right)\right]^{1/2}$$

- **Two parameters determine whether a bore will be generated from an intrusive gravity current:**
  - μ > 0.7 is required for bore
  - Solitary waves require large Froude Number

$$F = \frac{\left(U - C_{gc}\right)}{C_*} = \frac{\left(U - C_{gc}\right)}{\sqrt{g\Delta\theta\, d_0/\theta_{vw}}}$$

$$\mu = \frac{C_{gw}}{C_{gc}} = \frac{2Nh_0/\pi}{C_{gc}}$$

- **Vertical variation of the Scorer parameter determines likelihood of wave trapping**

$$m^2 = \frac{N_m^2}{\left(U - C_b\right)^2} - \frac{\partial^2 U/\partial^2 z}{\left(U - C_b\right)} - k^2$$

Complications

- **Gravity currents may generate other kinds of phenomena in addition to bores and solitons:**
  - **Kelvin-Helmholtz waves (strongly trapped waves that propagate rearward relative to the current head)**
  - **Trapped lee waves (display no tilt nor relative motion)**
  - **Intermediate structures during early stage of bore formation composed of some combination of current and inversion air**

- **Bore properties may not compare well with theory when:**
  - **Vertical wind shear is present**
  - **The inversion is elevated or stratification is complex**
  - **Gravity current is unsteady or multiply-structured**

IHOP_2002 (International H_20 Project) Surface Observing Sites

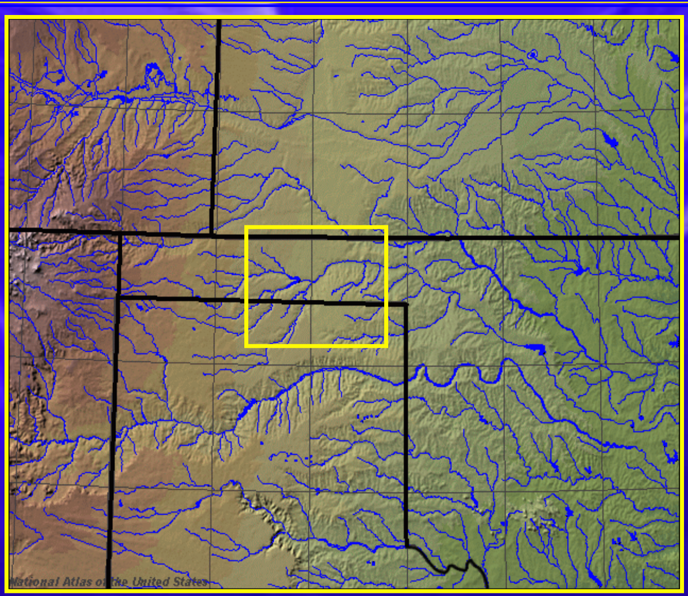

Homestead observing systems:

- ✓ S-POL Doppler radar with refractivity est.
- ✓ FM-CW 10-cm radar @ 2-m resolution
- ✓ MAPR (915 MHz Multiple Antenna Profiler @30-sec, 60-m resolution)
- ✓ HARLIE (aerosol backscatter lidar)
- ✓ GLOW (Doppler lidar)
- ✓ Scanning Raman Lidar @ 2 min, 60m
- ✓ AERI (Atmospheric Emitted Radiance Interferometer @10 min, 50m+)
- ✓ CLASS (3-hourly soundings)

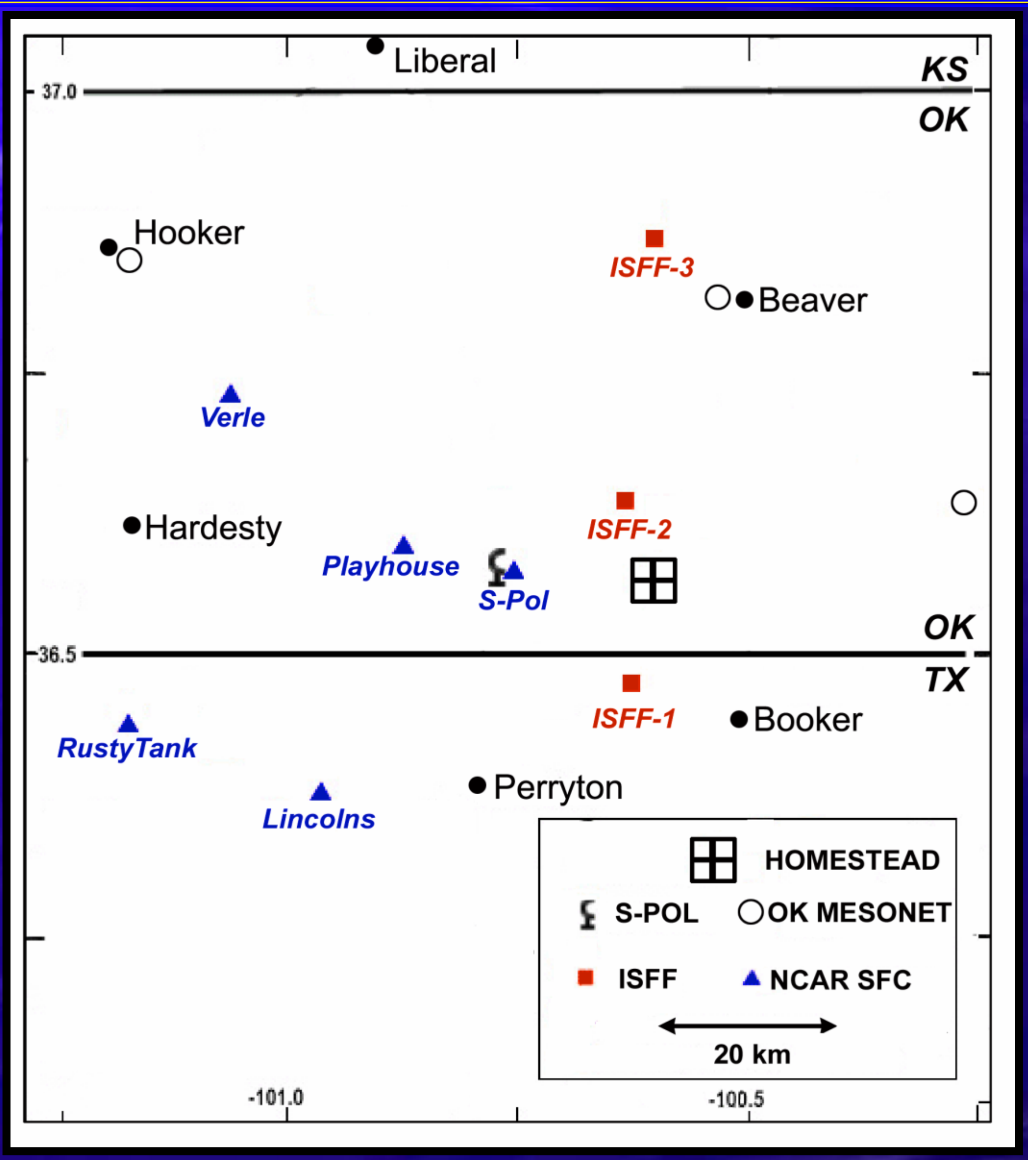

Generation of a Soliton by a Thunderstorm Outflow Boundary: June 20, 2002

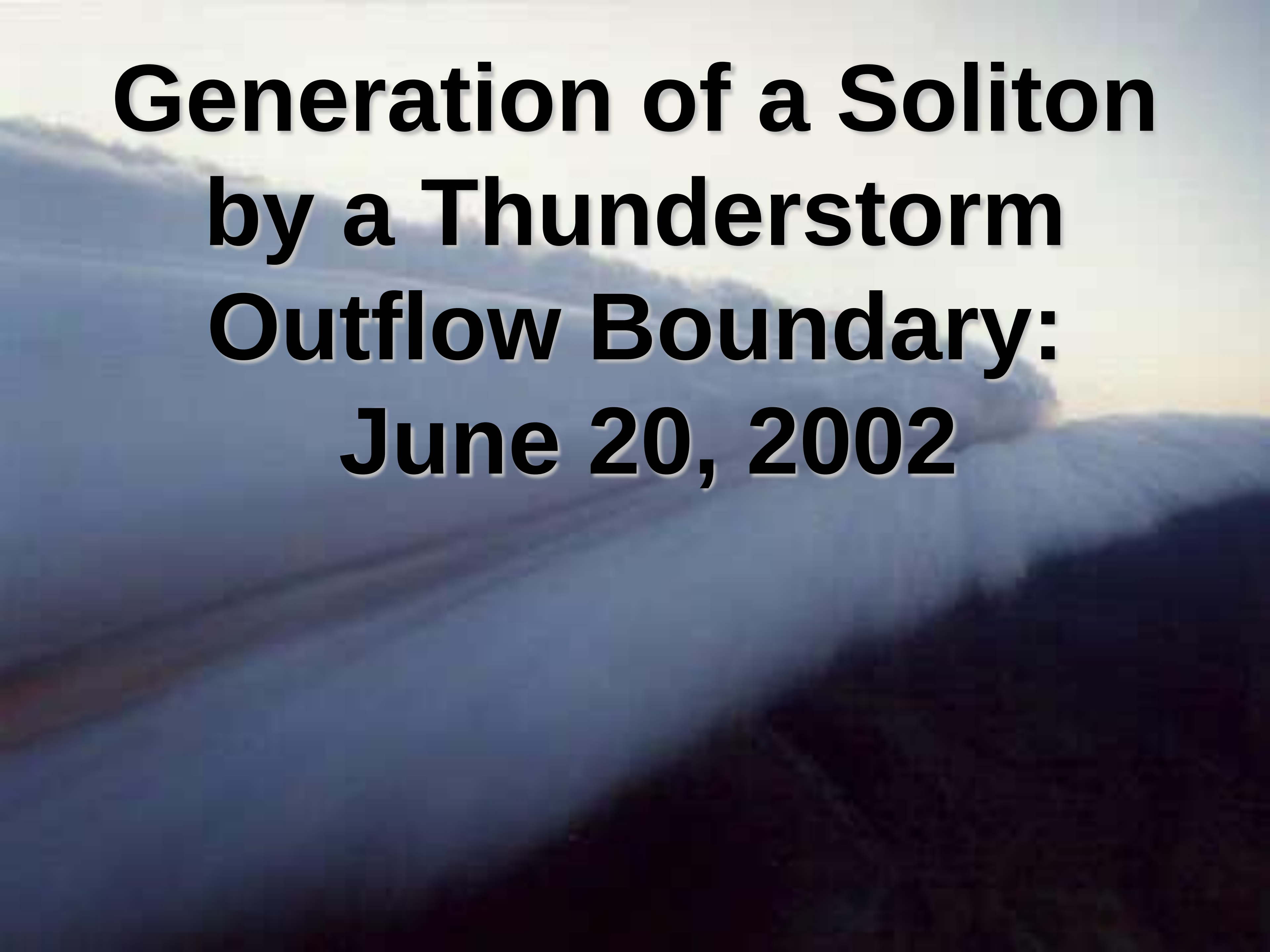

S-POL and DDC radar reflectivity + Surface Mesonet plot for 0036 UTC

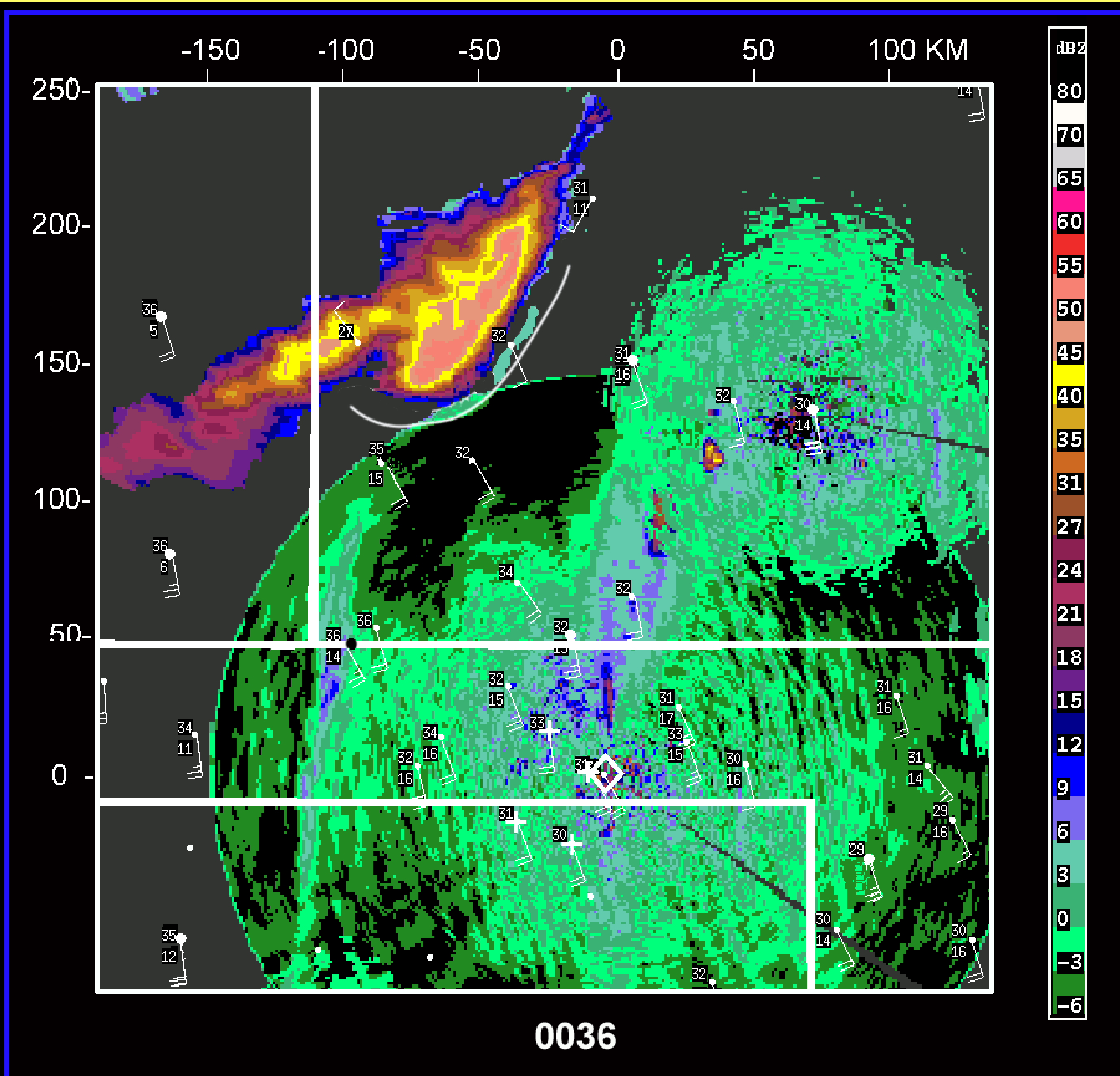

S-POL and DDC radar reflectivity + Surface Mesonet plot for 0233 UTC

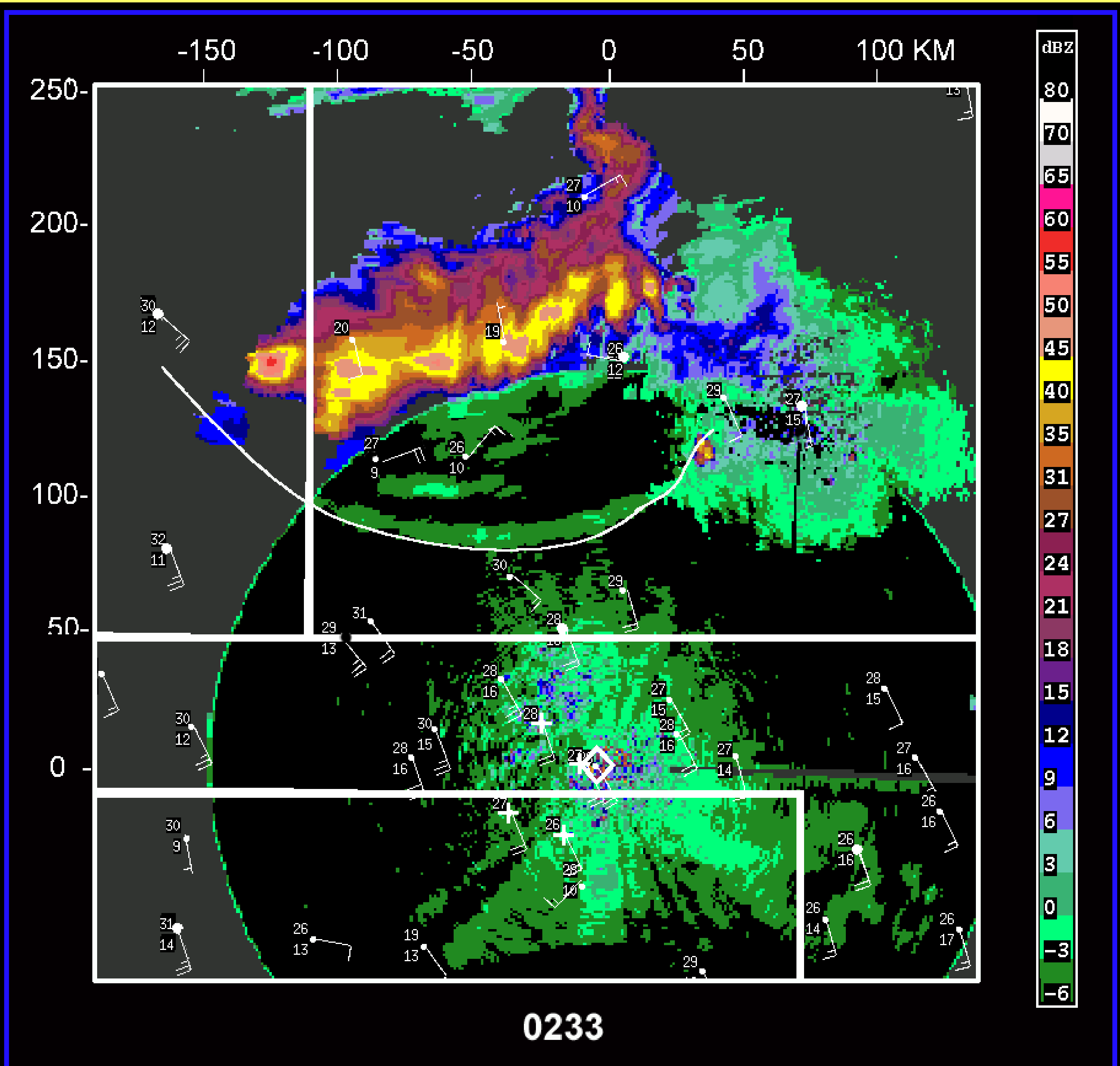

S-POL and DDC radar reflectivity + Surface Mesonet plot for 0533 UTC

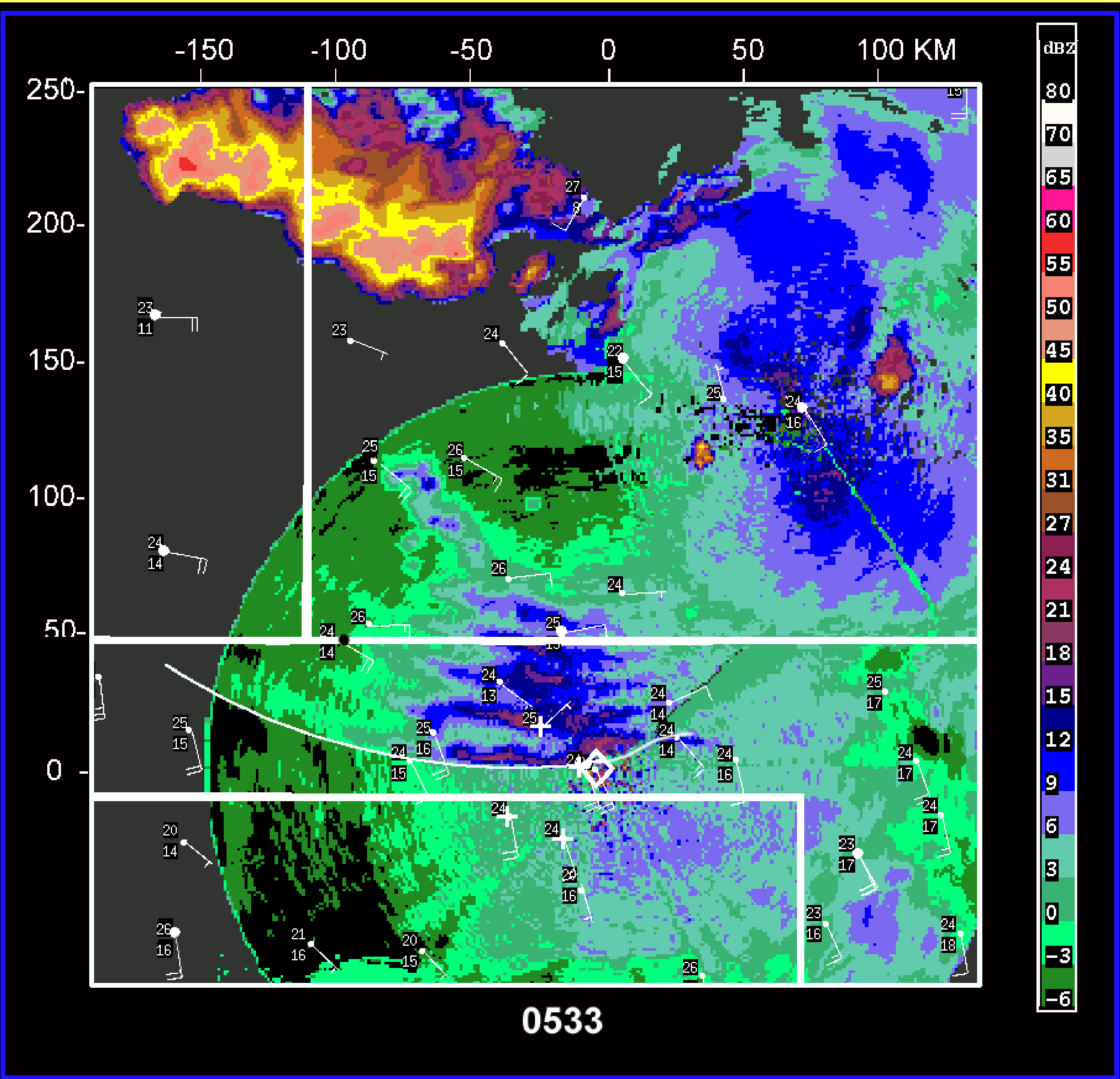

Displays: S-POL and DDC radar reflectivity + Surface Mesonet data

A fine line in the radar reflectivity fields is indicative of either Bragg scattering associated with pronounced mixing or Rayleigh scattering due to convergence of insects or dust.

Three different stages of the event:

- **Gravity current**: radar fine line + cooling + pressure increase
- **Bore**: 1 or 2 radar fine lines + **no** cooling + pressure increase
- **Soliton**: train of wavelike radar fine lines + no cooling + pressure increase

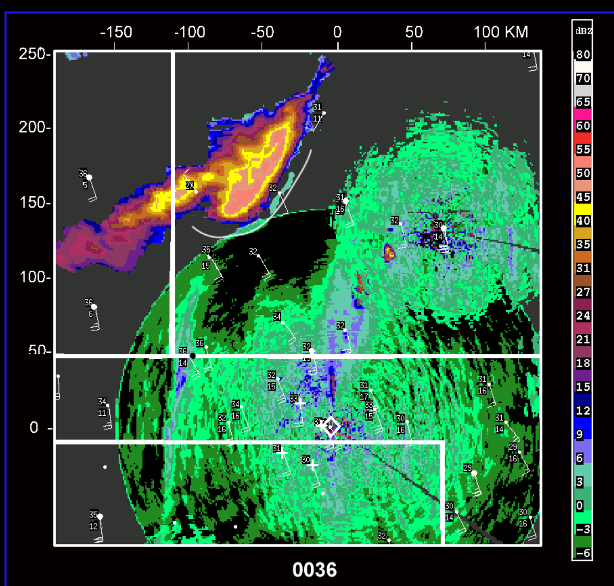

Gravity current

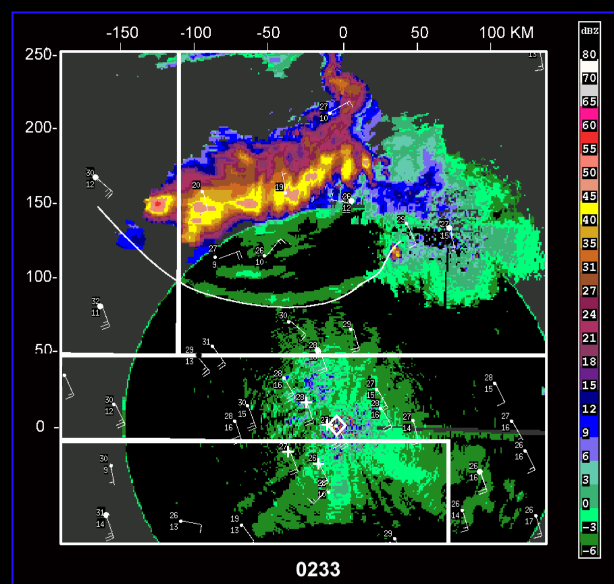

Bore

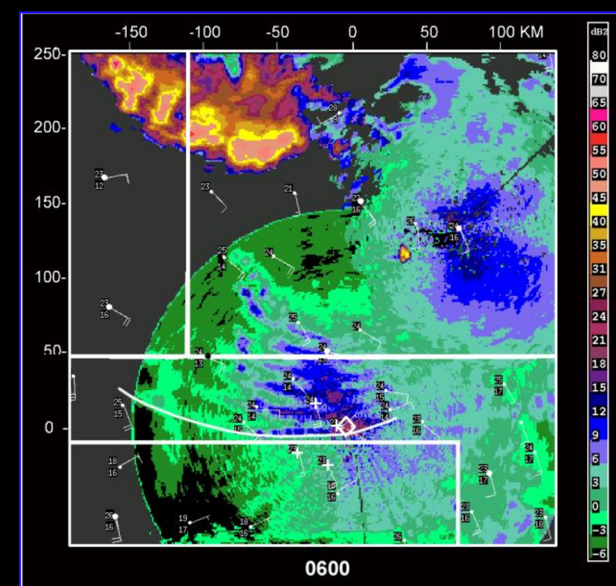

Soliton

Vertical structure of the bore as measured by Leandre2 DIAL water vapor system

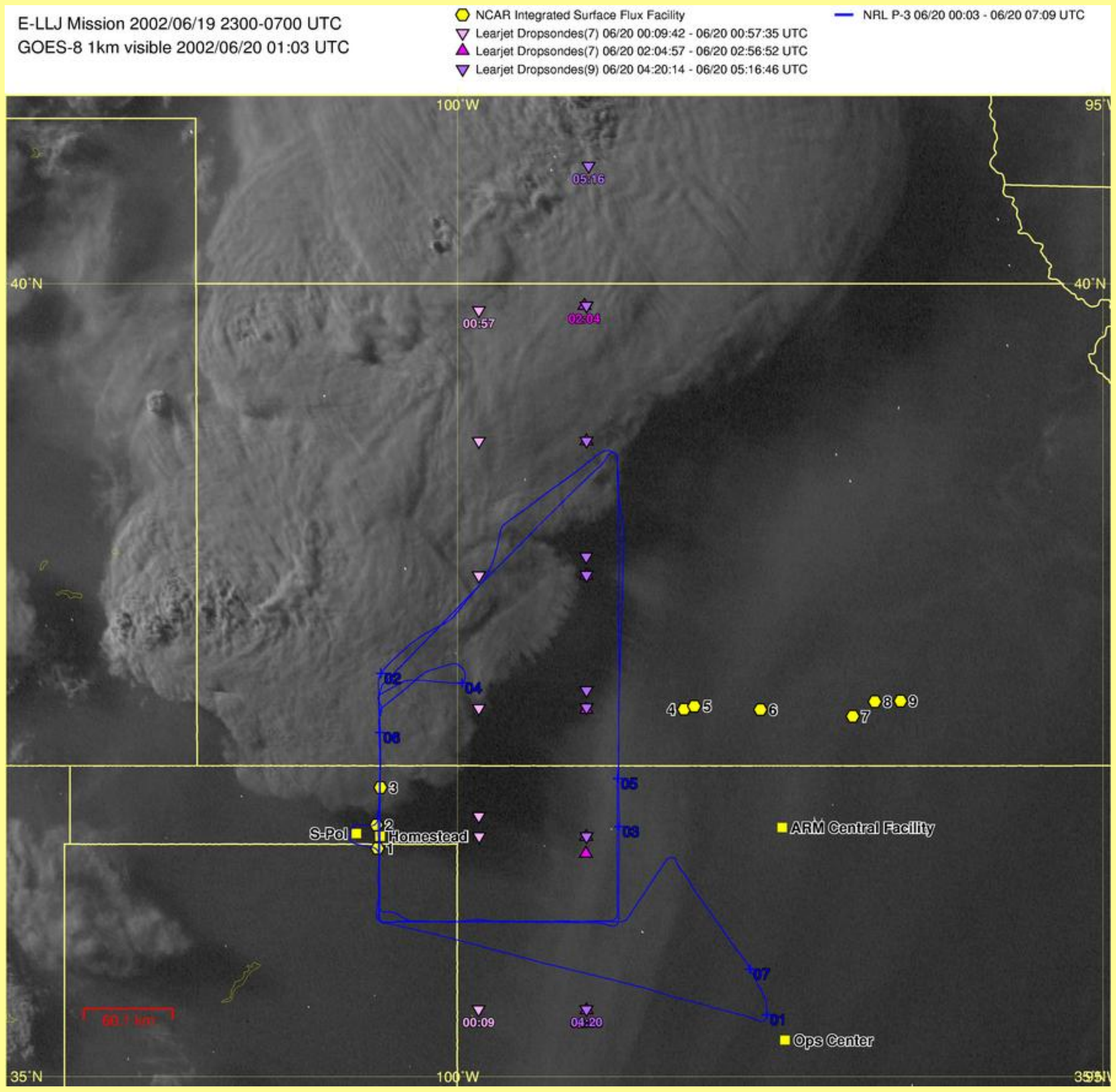

The evolution of the bore was observed by the LEANDRE 2 DIAL on the P-3 aircraft along N-S cross sections normal to the bore.

Four P-3 overpasses occurred over the Homestead Profiling Site, offering comparisons with S-POL, SRL, GLOW, MAPR

L2 WVMR retrievals:
800 m horizontal resolution
300 m vertical resolution

LEANDRE 2 : 3rd pass (0408-0427 UTC)

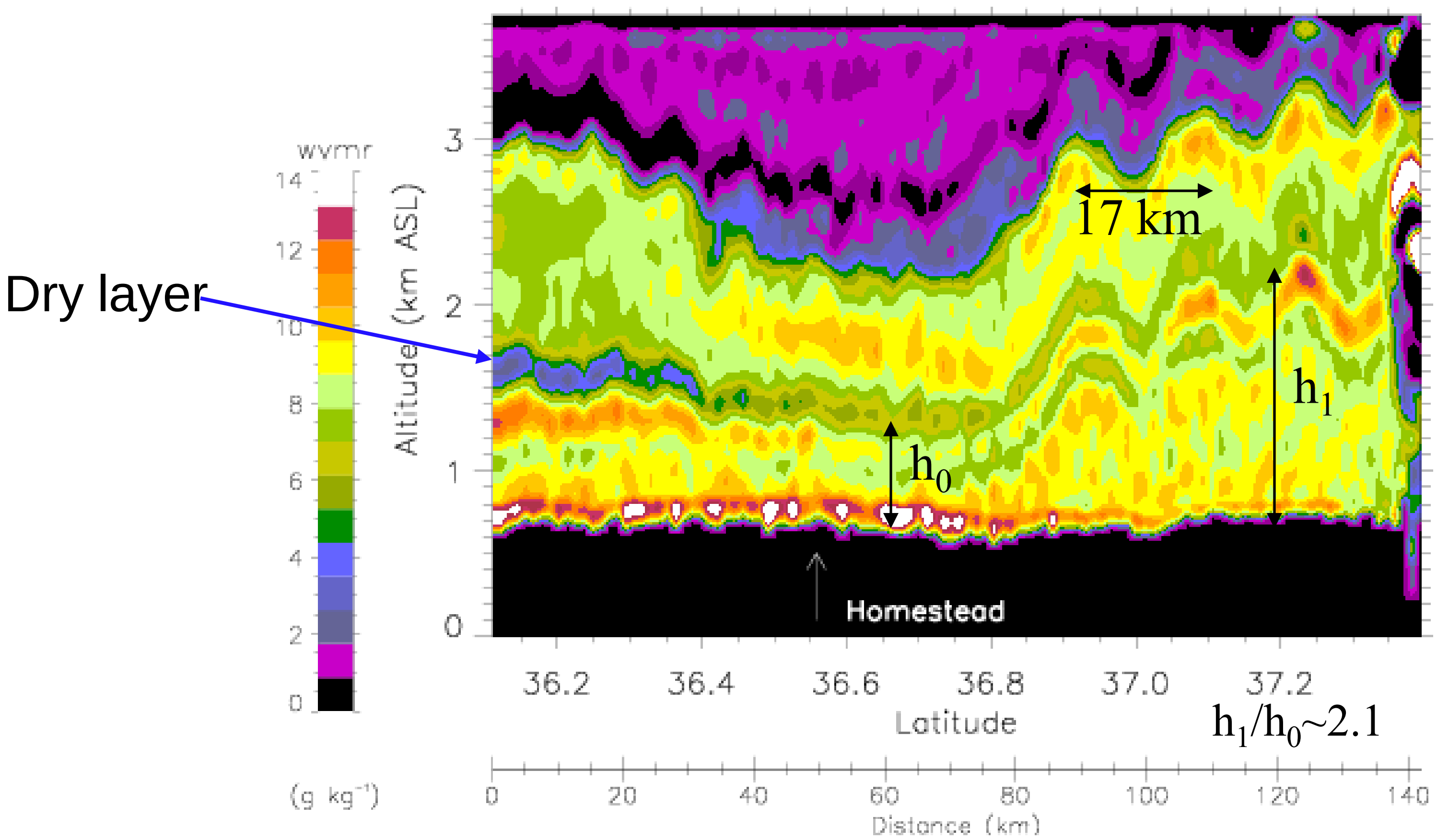

- Amplitude-ordered waves
- Inversion surfaces lifted successfully higher by each passing wave
- Trapping mechanism suggested by lack of tilt between the 2 inversion layers

LEANDRE 2 : 4th pass (0555-0616 UTC)

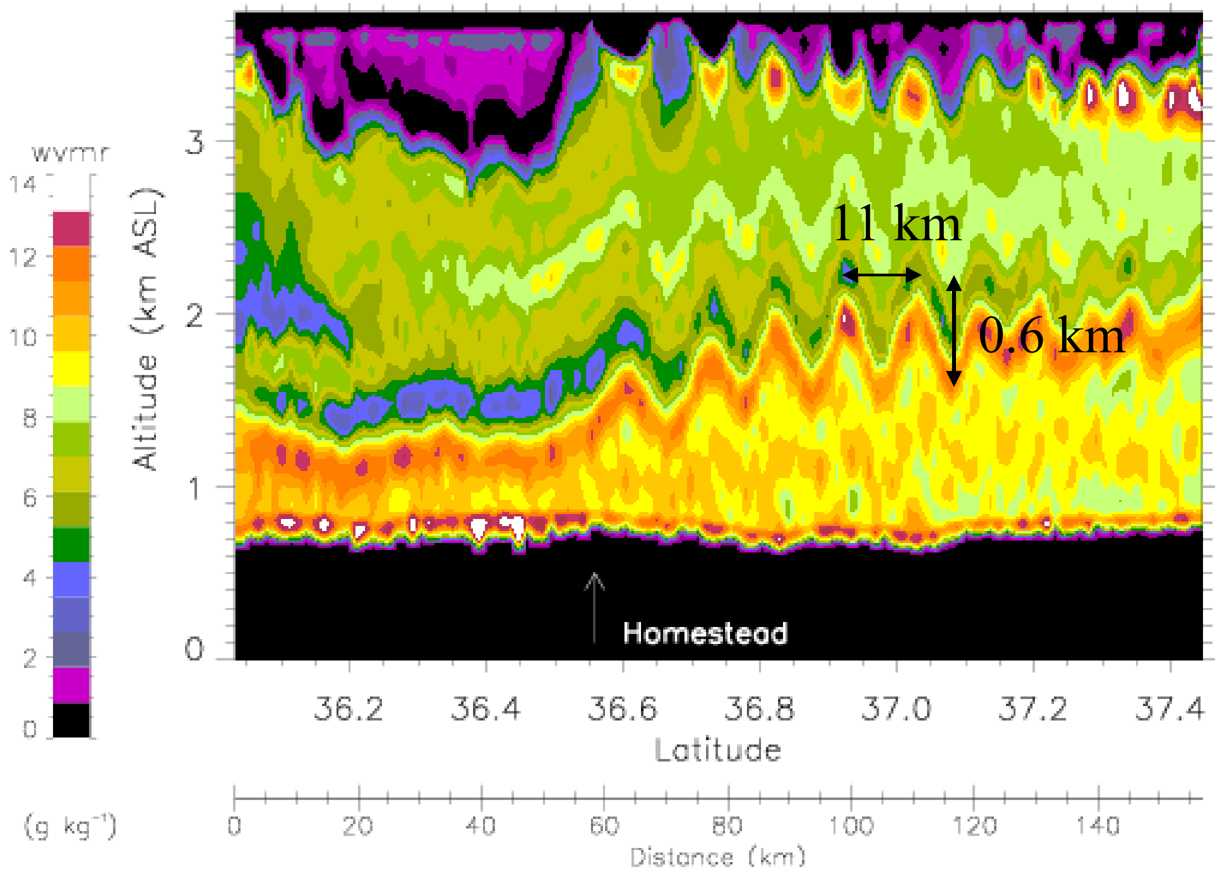

- Waves are no longer amplitude ordered
- Inversion surfaces lifted successfully higher by each passing wave
- Leading wave is weaker, but clouds have formed aloft above each wave
- Trapping mechanism suggested by lack of tilt between the 2 inversion layers

S-POL RHIs at 0530 UTC along azimuth 350°

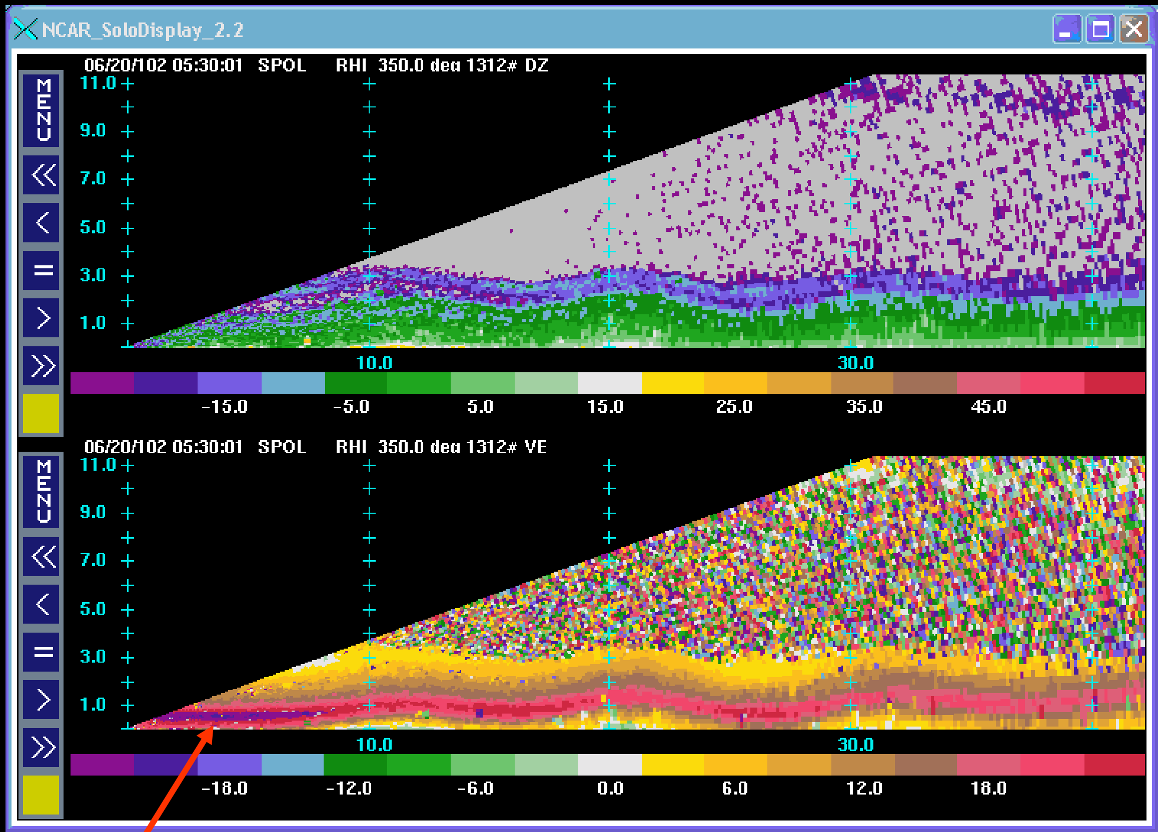

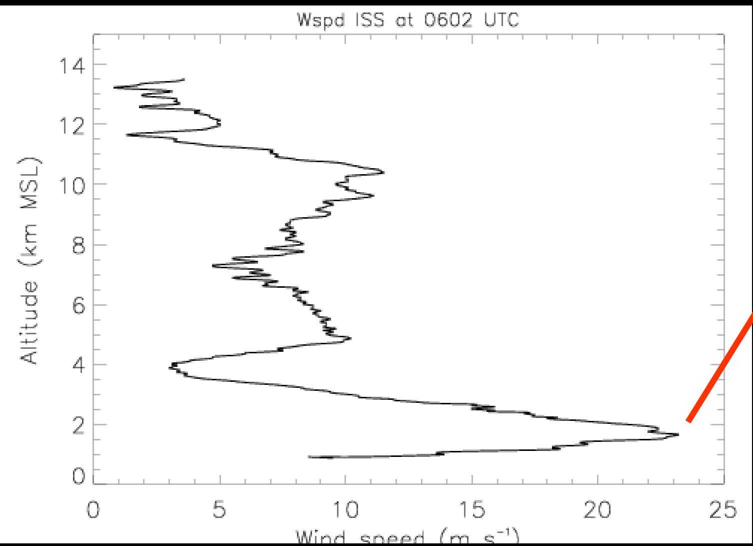

11-km horizontal wavelength at 2.5-km level and $22\ m\ s^{-1}$ LLJ seen in S-Pol data are consistent with Leandre-II and ISS observations, respectively

Representative Sounding for the Bore Environment seen in IHOP

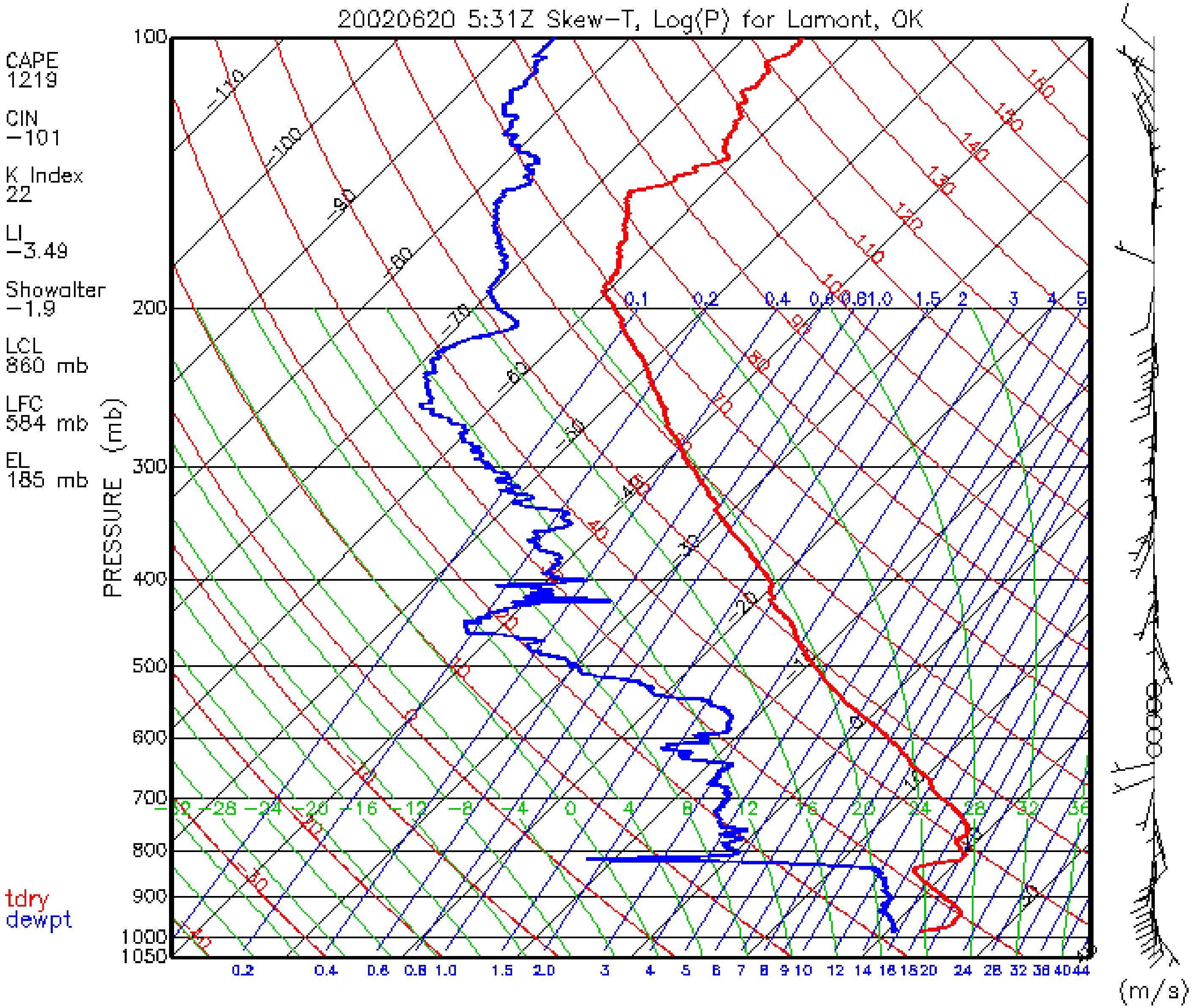

The Dual Bore Event on June 4, 2002

Pressure and Temperature 1-min Fluctuations Attending Passage of the Bores

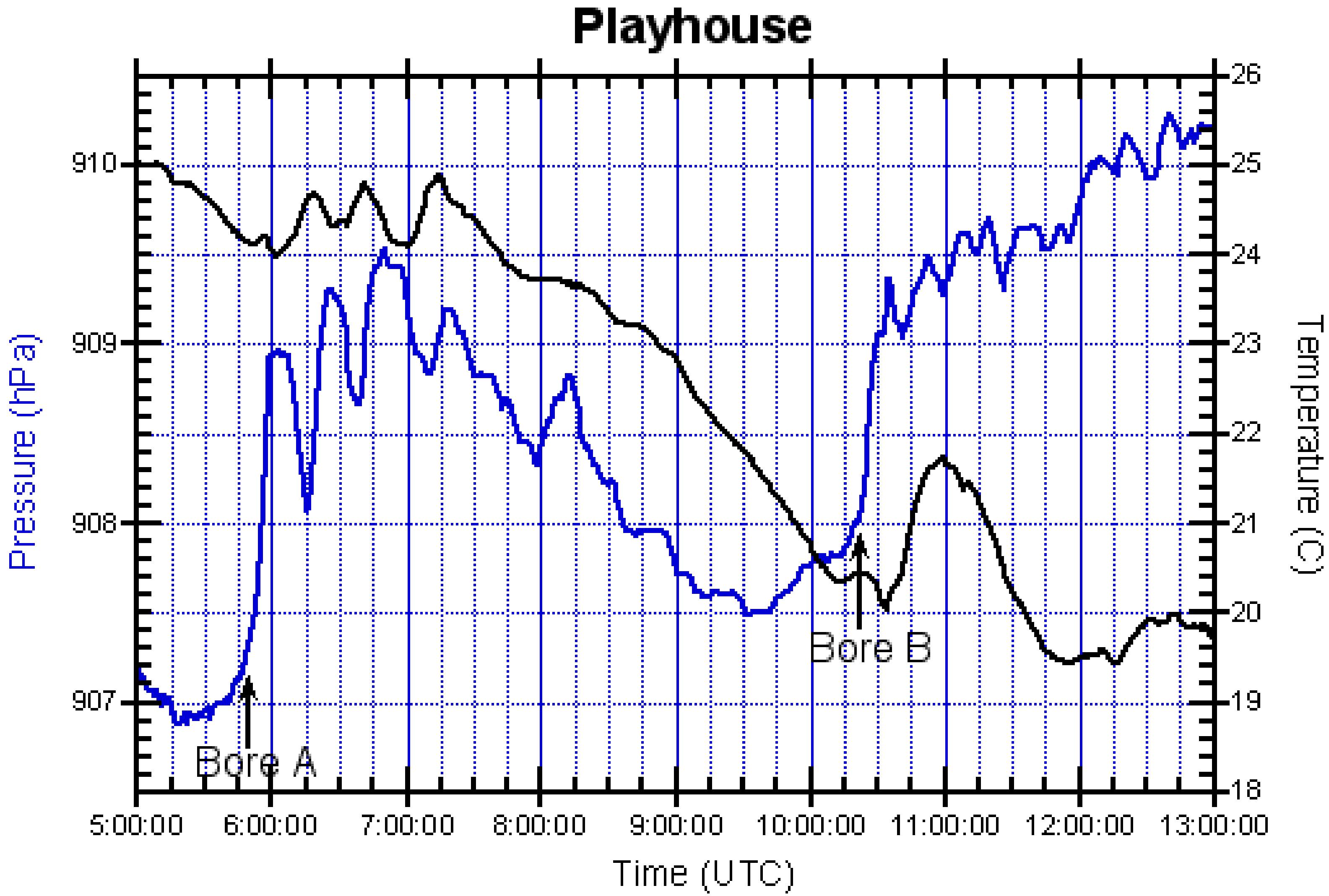

Warming or very slight temperature changes occur with passage of both bores

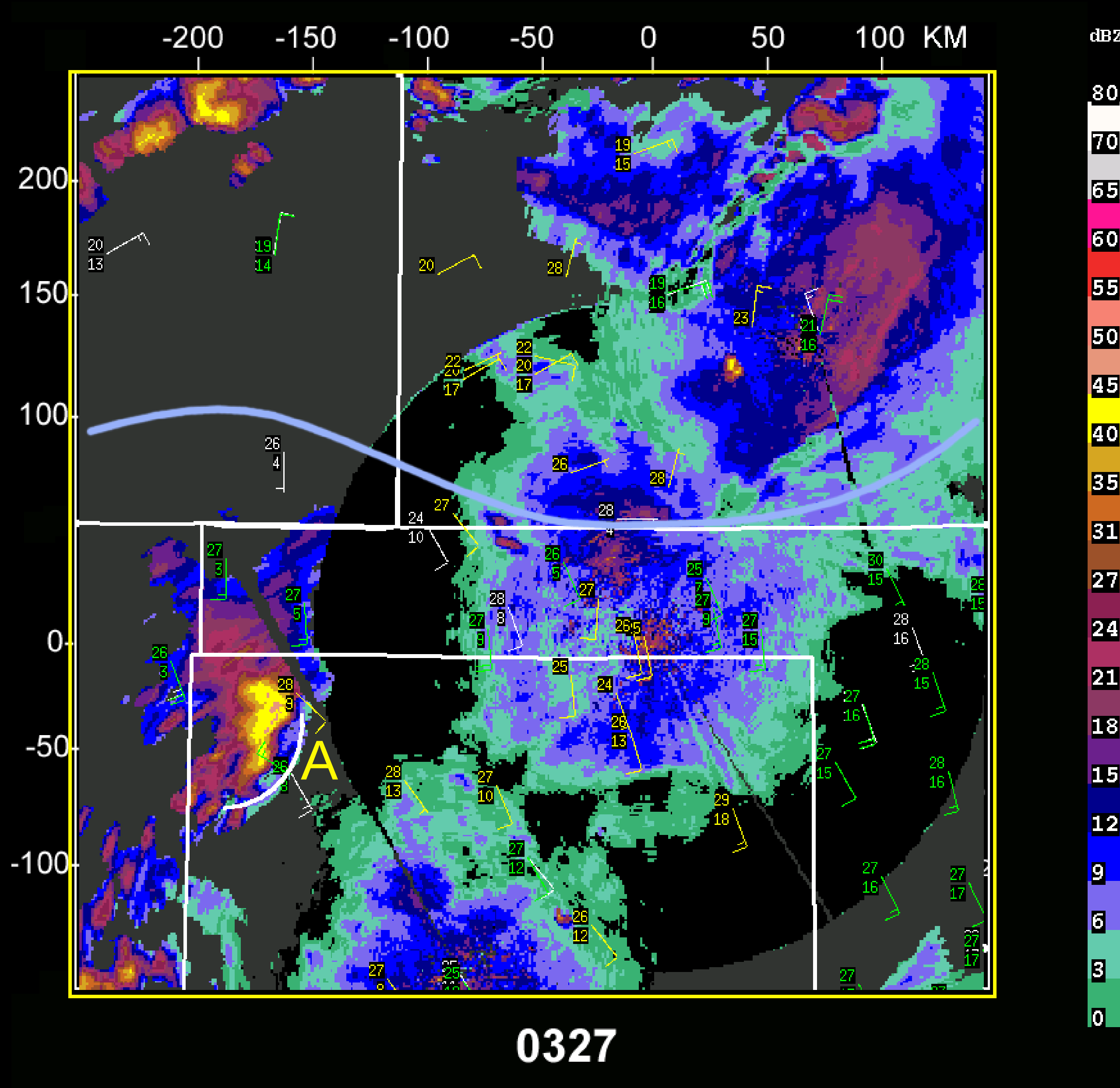

Evolution of gravity currents or bores (white lines) and synoptic cold front (blue line) as seen in Radar Composite and Mesonet Data

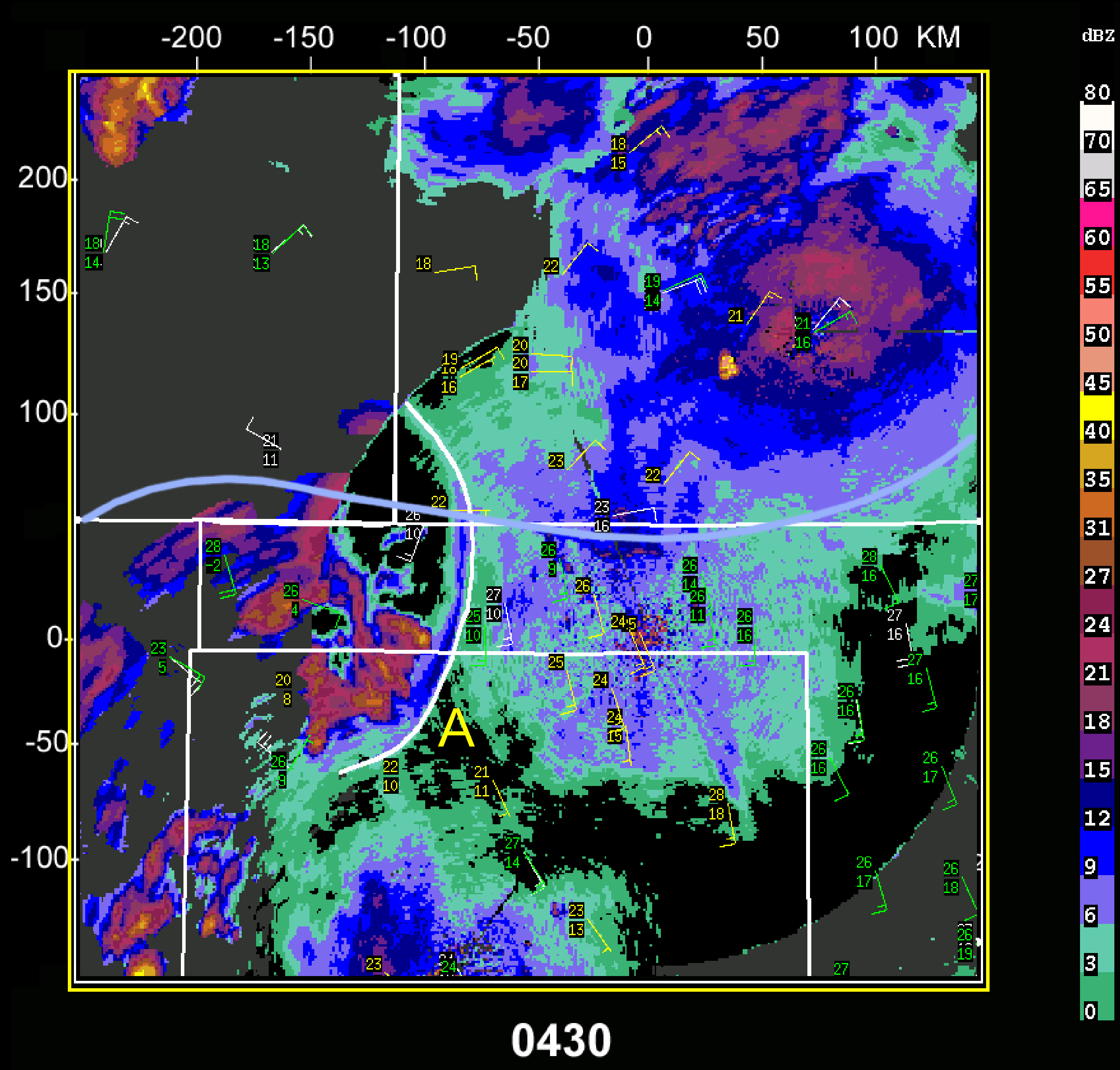

Evolution of gravity currents or bores (white lines) and synoptic cold front (blue line) as seen in Radar Composite and Mesonet Data

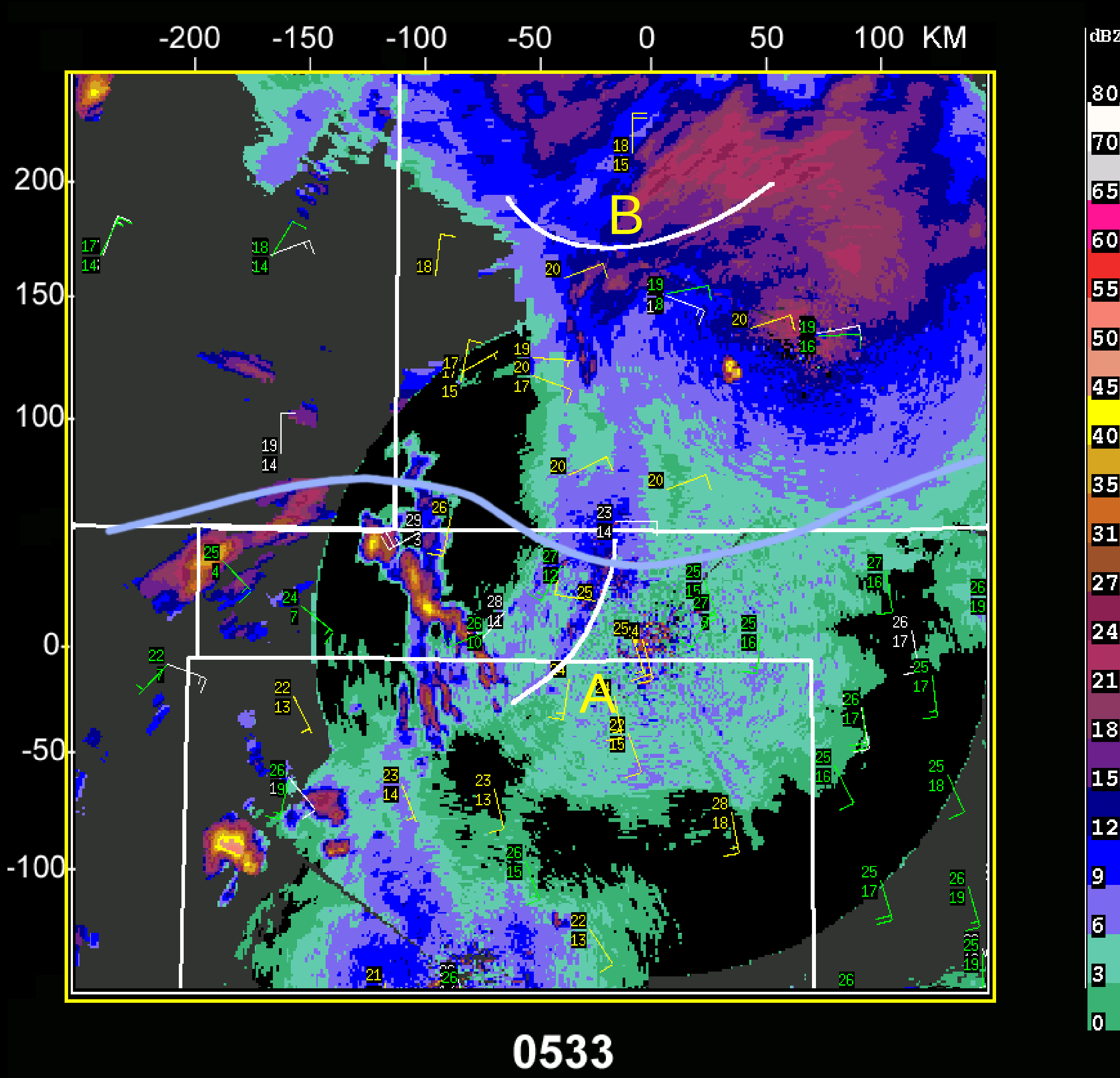

Evolution of gravity currents or bores (white lines) and synoptic cold front (blue line) as seen in Radar Composite and Mesonet Data

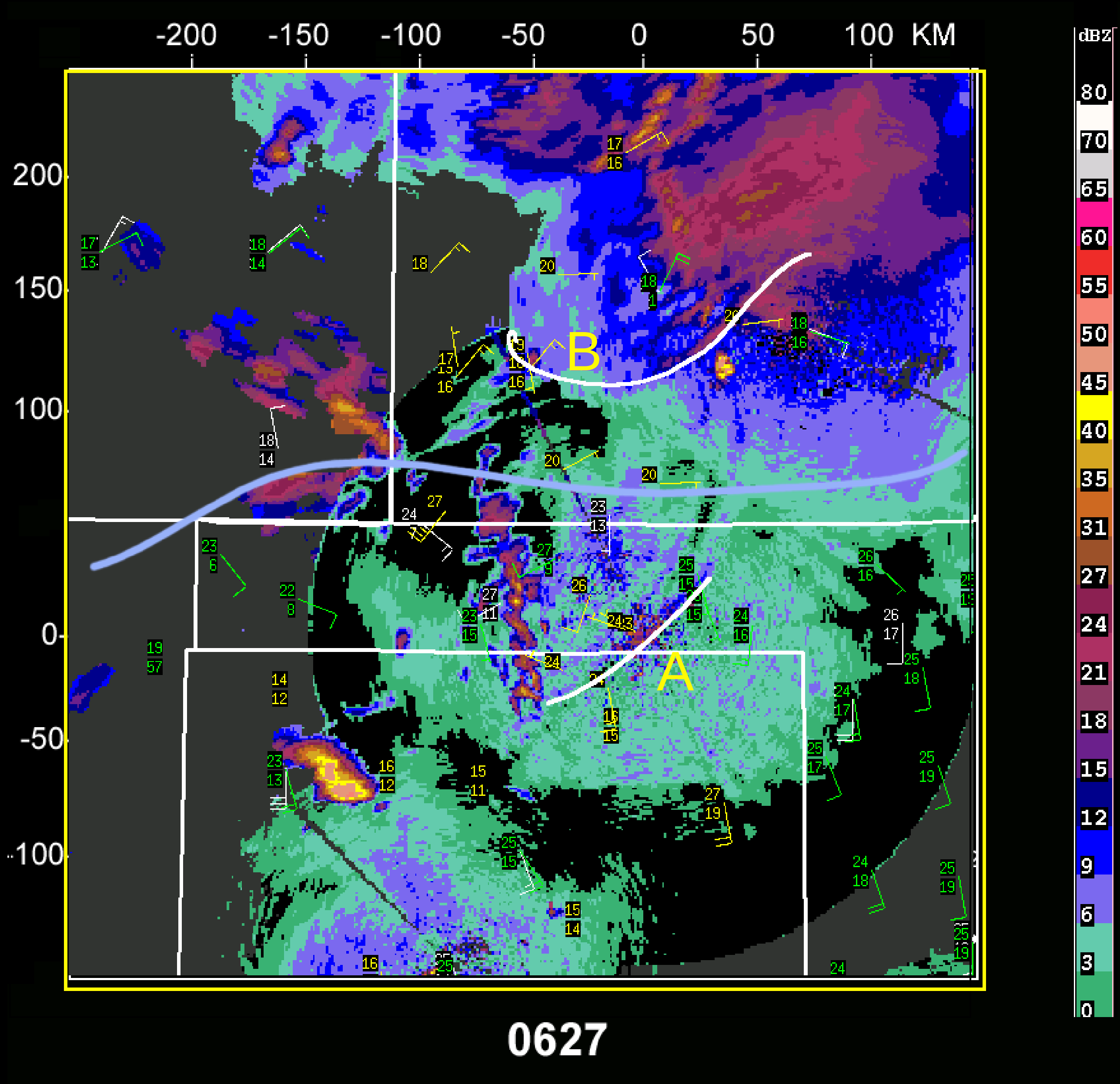

Evolution of gravity currents or bores (**white lines**) and synoptic cold front (blue line) as seen in Radar Composite and Mesonet Data

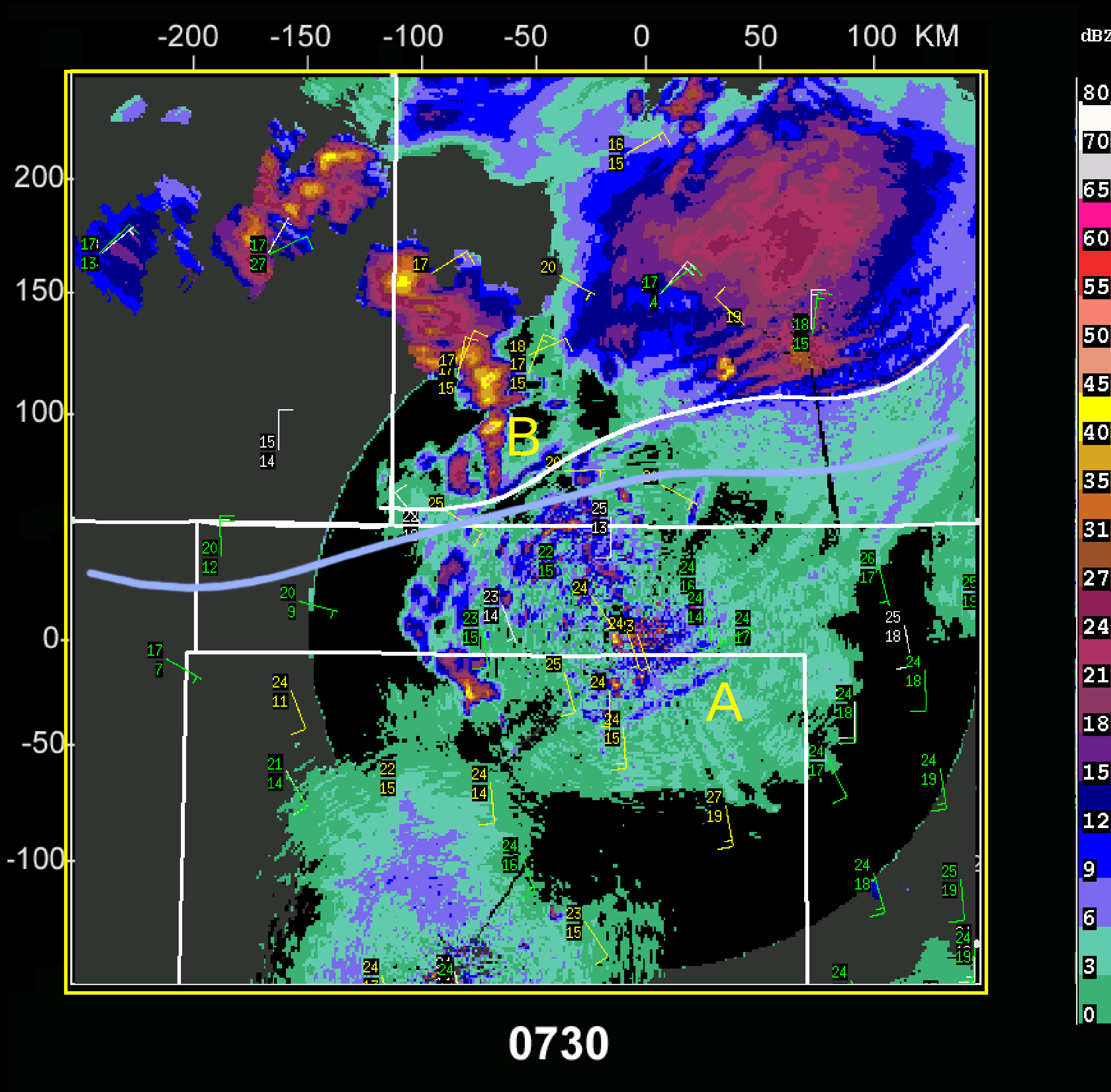

Evolution of gravity currents or bores (**white lines**) and synoptic cold front (blue line) as seen in Radar Composite and Mesonet Data

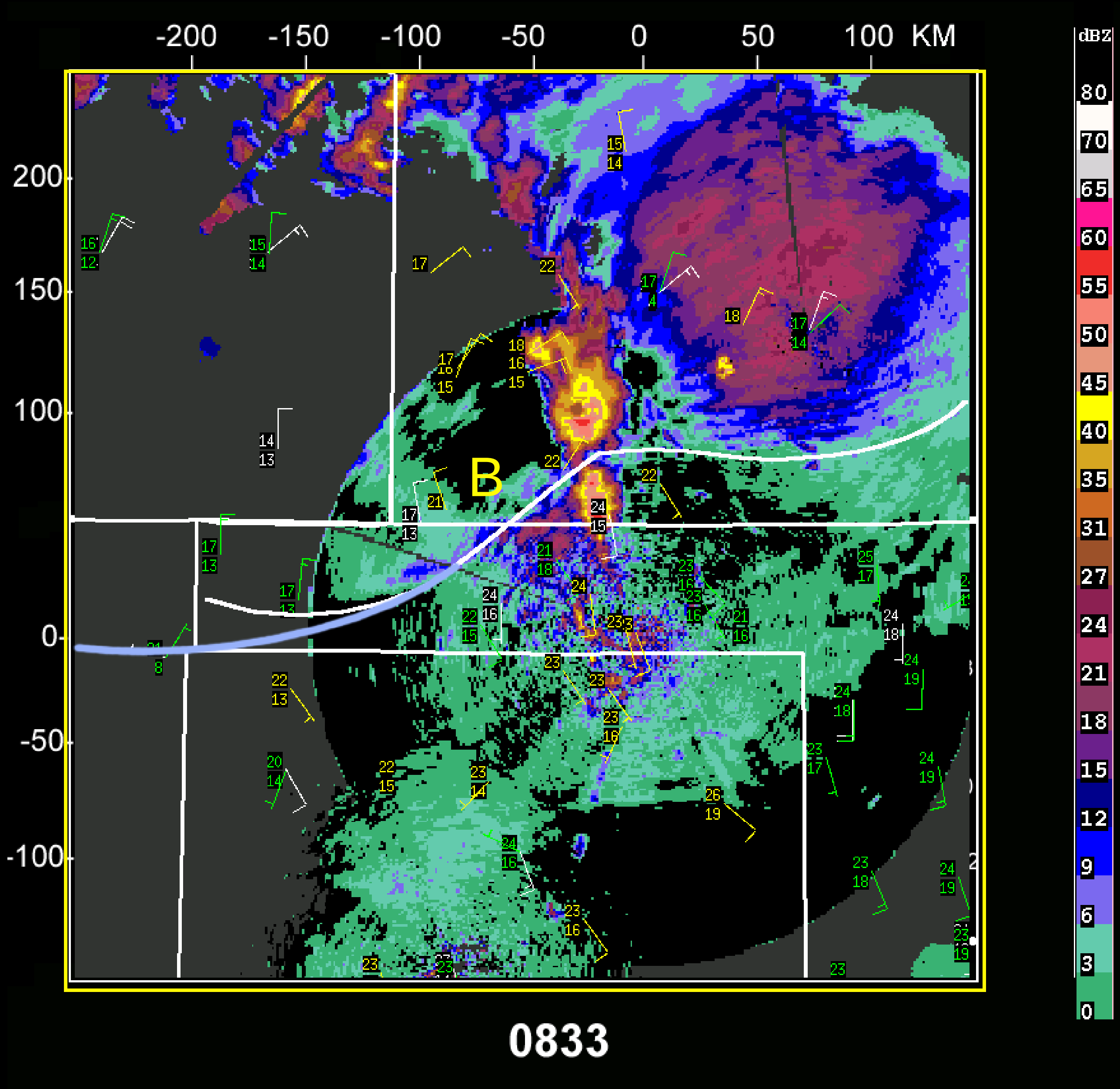

Evolution of gravity currents or bores (white lines) and synoptic cold front (blue line) as seen in Radar Composite and Mesonet Data

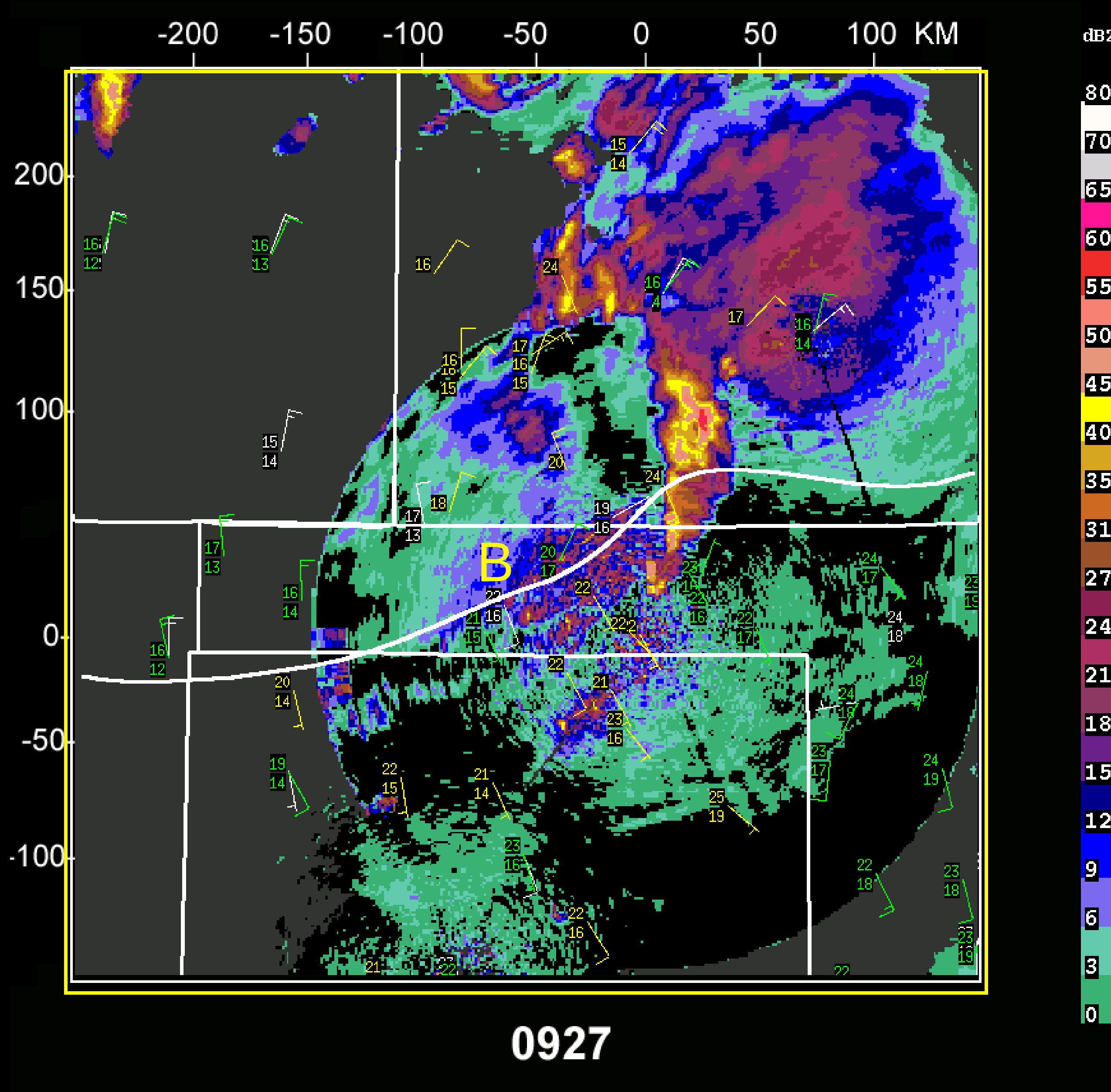

Evolution of gravity currents or bores (white lines) and synoptic cold front (blue line) as seen in Radar Composite and Mesonet Data

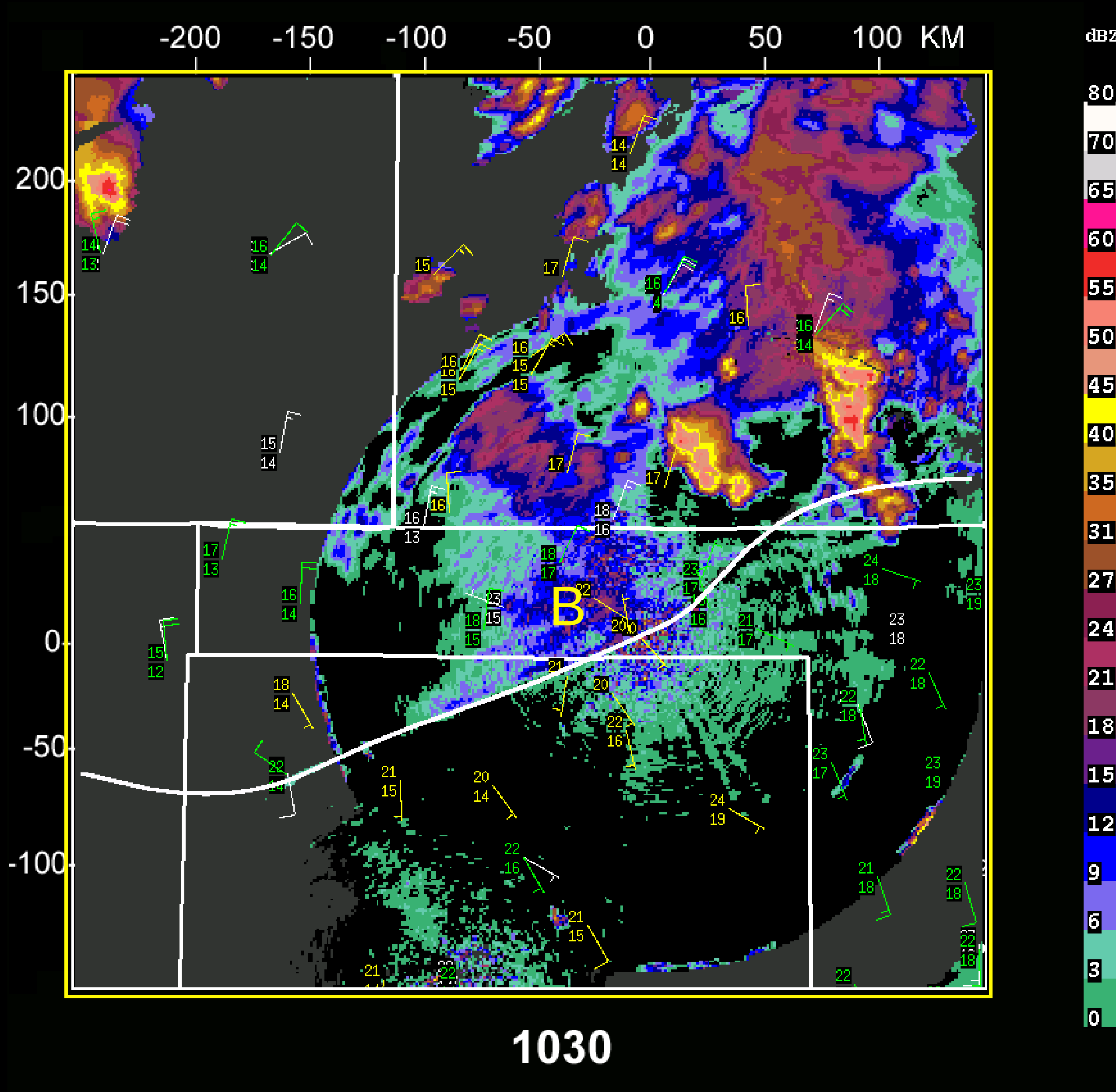

Evolution of gravity currents or bores (white lines) and synoptic cold front (blue line) as seen in Radar Composite and Mesonet Data

Bore A as seen by FM-CW and HARLIE

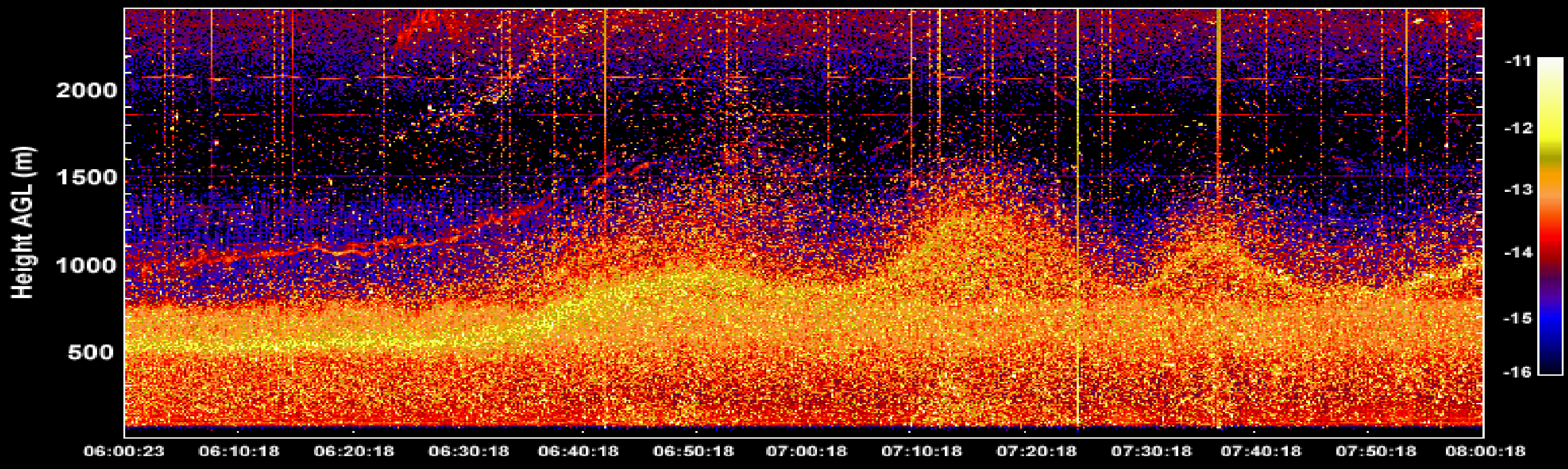

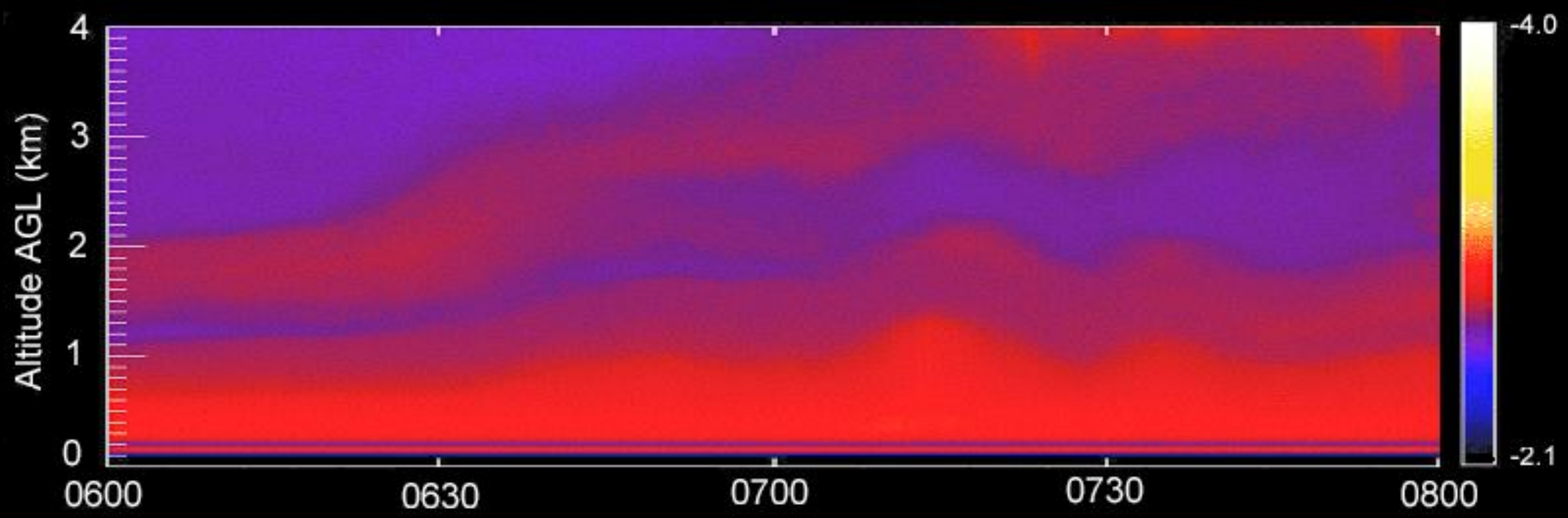

Bore A as seen by FM-CW and MAPR

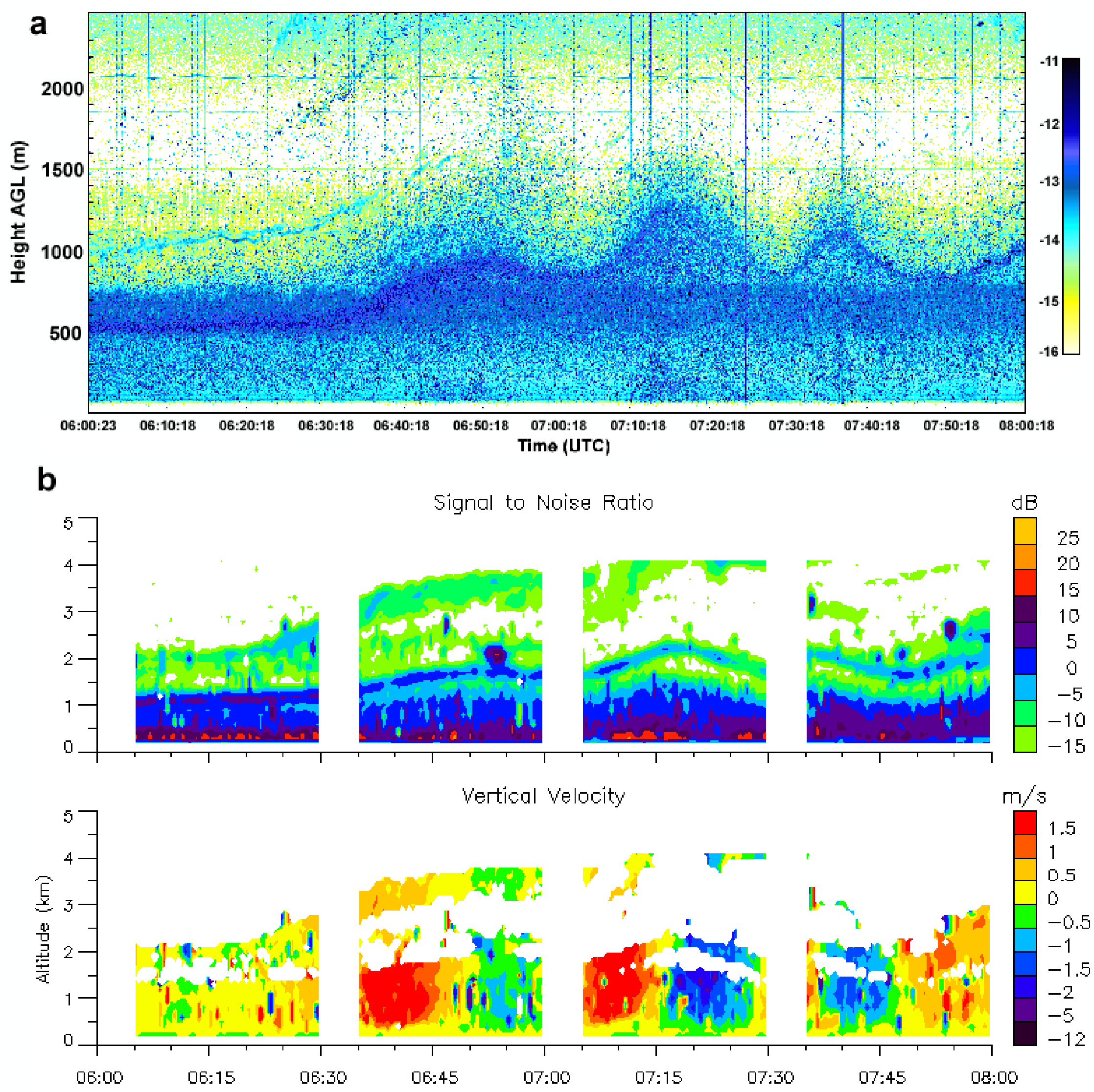

Bore B as seen by FM-CW and Raman Lidar

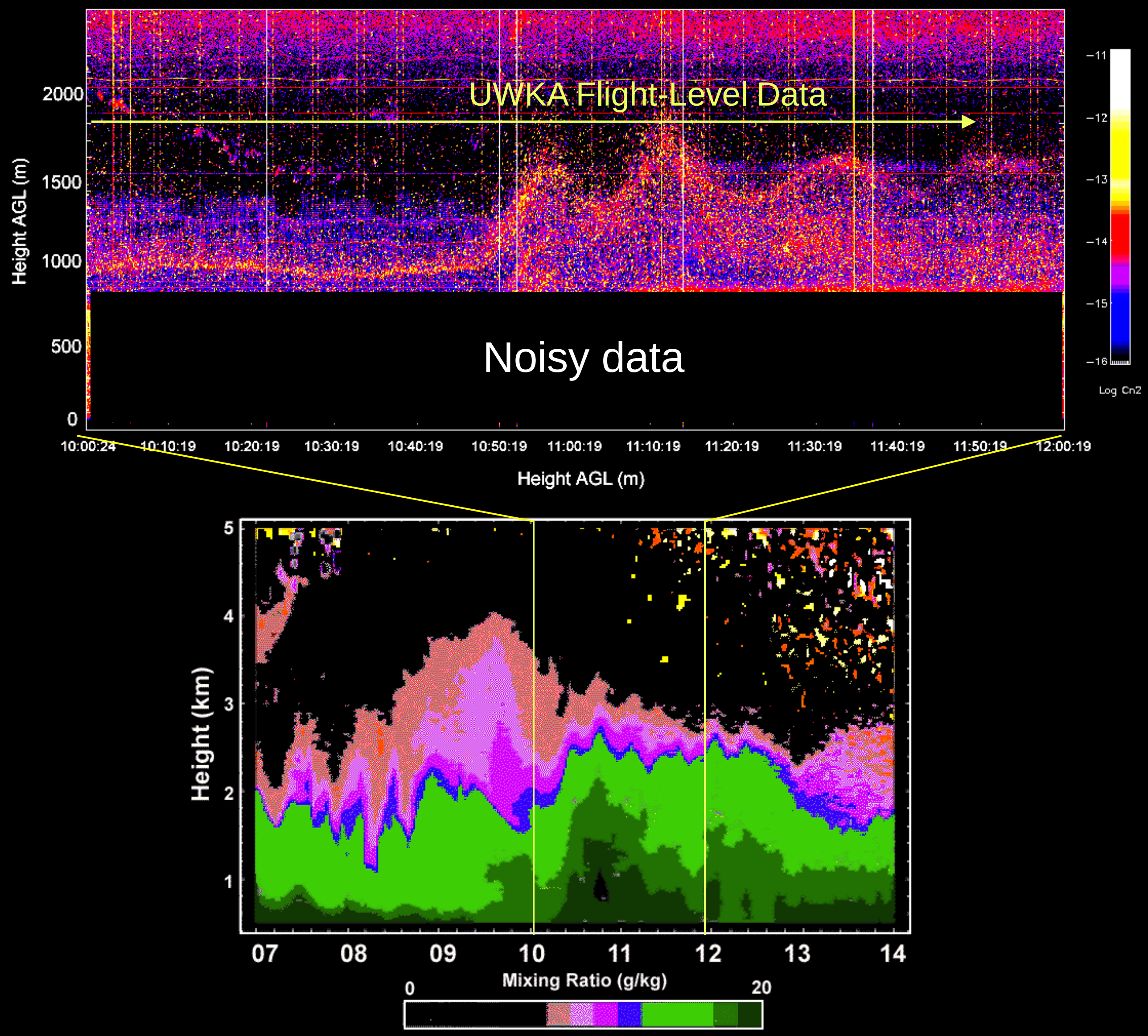

Bore B in UW King Air Data at FL1850 m AGL

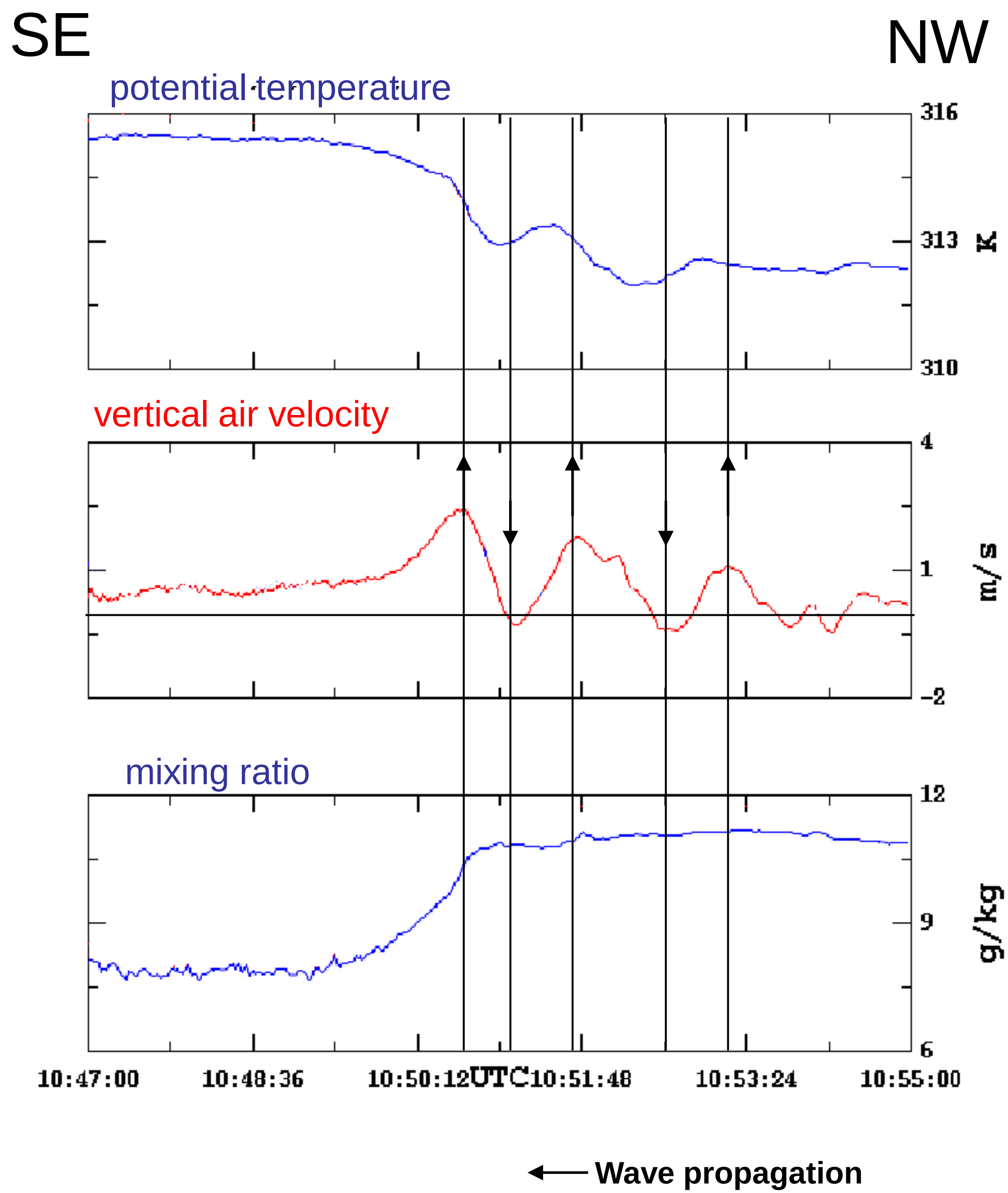

Bore B seen in UW King Air Data at FL 1850 m AGL

- **3C cooling and 4 g/kg more moisture are found at this level behind the bore (NW).**
- **Amplitude-ordered solitary waves were penetrated by the UWKA at the top of the bore.**
- **Vertical motions are in phase quadrature with q (upward motion leading cooling) and U (not shown), as in a typical gravity wave.**

Summary of Findings

➢Bores and solitons appeared as fine lines in S-POL reflectivity displays and their vertical structures were readily detected by lidar and radar systems (DIAL, Raman lidar, HARLIE, GLOW, LEANDRE2, MAPR, etc).

➢Solitary waves developed on a surface stable layer. The inversion was lifted abruptly by the leading wave and further by each passing wave, thereby destabilizing the atmosphere.

➢Nature of wave propagation did **not** suggest wave origin is intrinsic to bore dynamics as expected from bore theory, but rather, that “lee-wave” activity was the cause for the waves.

➢Solitary wave characteristics:

- ➢Horizontal wavelength: 10-20 km (4 June) 16 decreasing to 11 km (20 June)
- ➢Phase speed: 11.4 – 12.6 m/s (4 June) 8 decreasing to 5 m/s (20 June)
- ➢Waves exhibited amplitude-ordering (except in later stages of 20 June soliton)
- ➢Suggestion of wave trapping seen in Leandre2, Raman Lidar data

➢Pronounced reduction in refractivity occurred due to **drying** in the surface layer (June 4 only), but cooling & **moistening** seen aloft in both cases (AERI, UWKA data for Bore B on 4 June, Leandre on 20 June) was likely a result of adiabatic lifting. Attempting to simulate all of this.

➢An unprecedented set of observations has been collected on the time-varying structure of bores and solitons in IHOP: 18 bore events were logged during the six-week IHOP experiment, allowing for common aspects of their environment to be determined.